

GROWTH OF A SINGLE CRYSTAL RIBBON IN SPACE

**CASE FILE  
COPY**

Prepared under Contract No. NAS8-27807

F. A. Padovani

F. W. Voltmer

TEXAS INSTRUMENTS INCORPORATED

P. O. Box 5012

Dallas, Texas 75222

For

NASA-GEORGE C. MARSHALL SPACE FLIGHT CENTER

Huntsville, Alabama

# GROWTH OF A SINGLE CRYSTAL RIBBON IN SPACE

## FINAL REPORT

Contract NAS8-27807

### Period Covered

29 June 1971 through 13 April 1973

May 1973

By

F. A. Padovani

F. W. Voltmer

Semiconductor Research and Development Laboratories

TEXAS INSTRUMENTS INCORPORATED

P. O. Box 5012

Dallas, Texas 75222

1.

2.

3.

4.

5.

## ABSTRACT

During the period from 29 June 1971 through 13 April 1973, work was done under NASA Contract NAS8-27807 to investigate three critical technological areas associated with adapting the method of pulling single crystal silicon ribbon to a space environment.

Basic parameters such as the magnitude of the forces required and the coupling between thermal and force fields are discussed. The design of a ribbon puller is described, and the problems encountered are also discussed. The force fields in the vicinity of a coil have been characterized and results of attempts to pull ribbon are described. The results of the one experiment to grow a conventional float zone crystal in an external static magnetic field are presented.

1

2

3

4

5

## TABLE OF CONTENTS

<i>Section</i>	<i>Title</i>	<i>Page</i>
I.	SUMMARY AND CONCLUSIONS . . . . .	1
II.	TECHNICAL DISCUSSION. . . . .	5
1.	Theoretical Considerations . . . . .	5
A.	Field Penetration . . . . .	5
B.	Surface Pressure . . . . .	5
C.	RF Force Density . . . . .	7
D.	Force-to-Power Density Ratio . . . . .	9
2.	Puller Design . . . . .	13
A.	Mechanical System . . . . .	13
B.	Electrical System . . . . .	19
C.	Problems . . . . .	19
3.	Force Measurements . . . . .	21
A.	Introduction . . . . .	21
B.	Method . . . . .	21
C.	Axial Forces . . . . .	25
D.	Radial Forces . . . . .	27
4.	Ribbon Growth . . . . .	27
A.	Introduction . . . . .	27
B.	Two-Coil System . . . . .	30
C.	Single-Coil, Complex-Wound System . . . . .	32
5.	Solidification in a Magnetic Field . . . . .	34

## APPENDIX. DETAILS OF THE RIBBON PULLER

1

2

3

4

5

## LISTS OF ILLUSTRATIONS

<i>Figure</i>	<i>Title</i>	<i>Page</i>
1.	RF Skin Depth for Solid and Molten Silicon near the Melting Point	6
2.	Shapes used for Calculating Surface Pressure	7
3.	Coordinate System and Orientation of Conductor and Silicon Used in Calculation of Forces of Silicon Ribbon	9
4.	Sample Configuration for Infinite Slab Calculations	10
5.	Force-to-Power Ratio for an Infinite Sheet Between Two Conductors	14
6.	Low-Frequency Approximation of Force-to-Power Ratio as a Function of Ribbon Thickness	15
7.	Force on an Infinite Sheet Between Two Current-Carrying Conductors	16
8.	Power Dissipated in an Infinite Sheet Between Two Current- Current-Carrying Conductors	17
9.	Ribbon Puller System	18
10.	Silicon Ribbon Puller Without Control Panel	20
11.	Power Supply and Oscillator Outputs	22
12.	Torsion Balance for Measuring Axial Force	23
13.	Photograph of Torsion Balance for Measuring Axial Force	24
14.	Torsion Balance for Measuring Radial Force	25
15.	Measured Axial Forces on Molten Silicon	26
16.	Force as a Function of Melt Position Relative to RF Coil	28
17.	Measured Radial Dependence	29
18.	Normalized Radial Force versus Distance from Coil Edge	29
19.	Dual-Frequency Coil Arrangement	31
20.	Center-Tapped Power Coil	31
21.	Shaped Material Coils	33
22.	Dislocation-Free Silicon Growth in the Presence of a Magnetic Field	35
23.	Resistivity versus Length of Crystal grown in the Presence of a Magnetic Field	36

This report was prepared by Texas Instruments Incorporated under Contract NAS8-27807, Growth of a Single Crystal Ribbon in Space, for the George C. Marshall Space Flight Center of the National Aeronautics and Space Administration.

## SECTION I

### SUMMARY AND CONCLUSIONS

This report summarizes accomplishments during the period 29 June 1971 through 13 April 1973 on the National Aeronautics and Space Administration Contract No. NAS8-27807. The ultimate objectives of the work are to investigate three critical technological areas associated with adapting the method of pulling single crystal silicon ribbon to the environment of space. The three critical areas include the shaping of molten silicon into a rectangular cross section using a radio-frequency field shaping guide, the characterization of solid-liquid interface kinetics and solute redistribution, and the determination of the thermal stability requirements.

The program was, as initially conceived, divided into three tasks. The first task included the experimental determination of the optimum spatial arrangement of coils, current levels, and frequencies for pulling a rectangular cross section circular ribbon and the experimental simulation of a zero-gravity environment to check thermal and mechanical stability. The method which was to be used to simulate zero gravity was crucibleless horizontal zone melting in which levitation of the molten zone is effected by passing direct current through the melt crystal system while simultaneously imposing a magnetic field on the melt.

The second task was to characterize experimentally the chemical and structural microinhomogeneities and solute redistribution of those crystals grown successfully in a magnetic field. If insufficient material is grown under the first task, crystals pulled normally, with the exception of an applied magnetic field, will be used. The characterization of the material should be directed toward determining whether the artificial viscosity induced by an applied magnetic field simulates zero gravity and what benefits the absence of convection currents will provide.

In the third task, a mathematical analysis of the heat transfer effects was to be performed to ensure optimum thermal stability during ribbon growth.

It rapidly became apparent that these three tasks could not be achieved in the scope of a one man-year effort. Emphasis was therefore placed on the ribbon growth portion of the contract. The first months of the program were devoted to the design and fabrication of a ribbon puller and the

installation of support facilities. The design was based on previous experience at Texas Instruments and on information available in the literature. Several problems were identified with attempts to pull ribbon from the puller. The most significant of these was the lack of characterization of RF forces acting on molten metals. Primary effort was therefore directed toward the characterization of these forces.

The initial concept of the experiment involved the induction heating of a feed bar at approximately 1 MHz and the shaping of the ribbon, as suggested in the literature, by a coil designed to provide antiparallel current paths on opposite sides of the ribbon. Using such a configuration, however, had several inherent difficulties. The use of two independent coils at the high potentials, which are required, produced arcing before sufficient power could be delivered to the silicon. In addition, the antiparallel coils provided insufficient forces to shape the material, probably because of the weakness of the RF magnetic field in the vicinity of the silicon. As an alternative approach, a new coil design was developed which produced measurable lateral forces on both solid and molten silicon. The difficulty encountered with the proposed particular coil configuration, however, was the large spatial dimension over which the RF shaping interaction occurred.

A second difficulty which was identified is that of arcing between different coils or between regions of high potential difference on the same coil. While this is not a particular problem in air, the oxide which forms in air forms a crust over the molten zone which prevents RF shaping. Thus, it was necessary to grow in an inert atmosphere such as argon. The low breakdown voltage of argon causes arcing if two generators are used and therefore it would be desirable to use a method other than induction heating to form a molten zone on the silicon rod. An alternative approach would involve using a single coil for both melting and shaping the silicon. The problems associated with this technique will be discussed. Reducing the RF potential to prevent arcing is not a viable solution in that high currents would be required to provide sufficient power. The losses in the coils would then become large, especially at the frequencies required for either the heating or shaping. Isolation of the feed bar prevents arcing between the coil and feed bar, while arcing between coils is a more difficult problem to overcome.

Some of the tradeoffs which must be considered in the RF shaping of molten silicon are discussed. The RF forces which are generated originate because of an interaction between induced currents and the electromagnetic-magnetic field. The strength of the interaction depends on the magnitude of the rms magnetic field and the induced current, both of which are dependent on the geometrical configuration of the system. In addition, there is power lost within the material which depends on the material properties, the induced current, and the geometrical configuration of the system. These two effects behave differently according to frequency and/or geometry. There are three regions to be considered, depending on the frequency and sample dimensions.

The three regions may be defined by the electromagnetic wavelength in the sample as follows:

- 1) If the wavelength is greater than a characteristic length of the sample, then there is neither heating of the sample nor RF forces on the sample
- 2) If the wavelength is near the characteristic length of the sample, then RF forces are present but the induction heating is weak and inefficient
- 3) If the wavelength is short, compared with the sample dimensions, then the heating is efficient, but the RF forces are reduced because of the difficulty in obtaining high magnetic field strength.

Since heating and shaping both depend on frequency independently of one another, the ideal situation would provide independent control of the induction coils and shaping guides. One approach would involve separate coils for shaping and heating. However, two RF coils in such close proximity to one another as is required, and at such high potentials, would not only be shunted by the silicon but also discharge to one another. An alternative approach involves using a single generator to supply a complexly wound coil. Using such a coil to both melt and shape the silicon would require a fortuitous choice of coil design, power and frequency, and would only apply for a given feed rod diameter and for ribbon of specific cross-sectional dimensions. To achieve both thermal and mechanical stability, along with the desired ribbon form, would be nearly impossible.

However, if a single coil is to be used in order to have sufficient parameters as variables to control both the heating of the molten zone and the shaping of the ribbon, it would be necessary to drive the coil at two different frequencies. This technique has its own drawbacks, requiring good RF isolation of the two oscillators as well as a stable variable frequency oscillator to prevent the signal of one oscillator to excite unwanted oscillations in the second oscillator

A third approach, to heat the sample by means other than induction heating, might provide a viable solution, since the power and frequency of the RF generator could then be altered to control the RF forces on the molten silicon.

There is no experimental verification of controlled RF shaping of molten metals in the literature. Unintentional shaping is achieved on levitation of molten metals because of the nonuniform forces induced by the particular coils used. Even for the case of levitation of solids, the quantitative measurements are limited to the weight of material suspended. It is only for the simple coil configuration that forces on solids, as a function of sample position, have been measured and compared with theoretical predictions.

We have determined the axial and radial forces on a molten cylinder of silicon. The results indicate that sufficient forces can be developed to achieve shaping, however the stability, control, and efficiency of the experimental configuration used was not adequate for space experiments. In addition, only limited shaping was achieved.

These results indicate that the direct-coupled single-turn coil will not meet the efficiency requirements imposed by the power available on a spacecraft. It is believed that the major source of inefficiency resides in the inability to produce large circulating currents with a small amount of RF power. The situation could be improved by the use of a short-circuited shaping guide coupled to an RF driving coil. It is recommended that further investigation be directed to the characterization of forces created by the short-circuit transformer. Both radial and axial forces should be characterized and the power required to achieve the desired forces should be determined. Based on such information, a decision to pursue the effort could be made.

## SECTION II

### TECHNICAL DISCUSSION

#### 1. THEORETICAL CONSIDERATIONS

##### A. Field Penetration

The skin depth of RF fields on silicon as a function of frequency is calculated from the expression

$$\delta = \sqrt{\frac{1}{\pi \mu \sigma \omega}}$$

The skin depth for both solid and molten silicon near the melting point is plotted as a function of frequency in Figure 1. The driving frequency of the shaping guides is determined by the desired penetration depth. To pull a ribbon 0.020-inch thick, the penetration depth should be approximately 5 mils, corresponding to a frequency of 15 MHz.

##### B. Surface Pressure

The surface pressure required to change the curvature of the melt is derived from Laplace's formula.

$$p = \gamma \left( \frac{1}{R_1} + \frac{1}{R_2} \right)$$

where

$p$  = surface pressure

$\gamma$  = surface tension

$R_1$  and  $R_2$  = principal radii

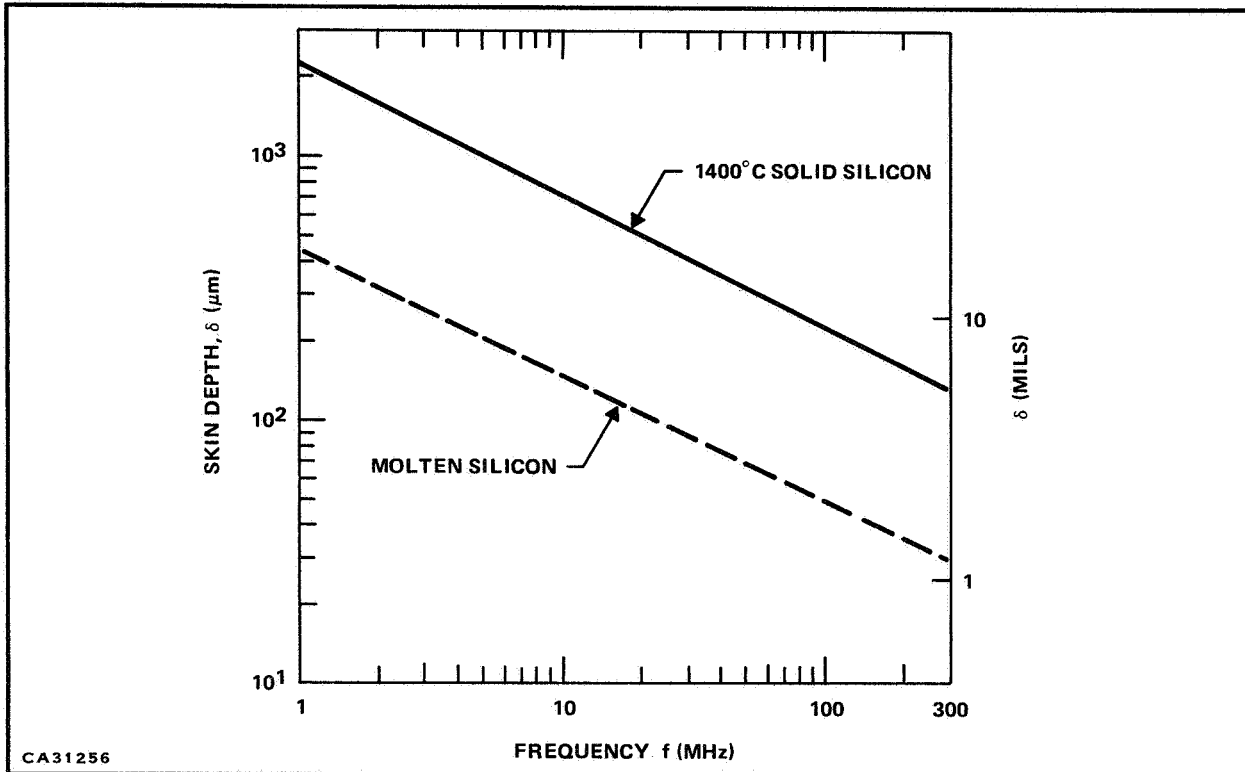


Figure 1 RF Skin Depth for Solid and Molten Silicon near the Melting Point

The pressure which must be applied to a cylinder to shape it into a ribbon is then

$$\Delta p = \gamma \left( \frac{2}{t} - \frac{1}{R_1} \right)$$

where

$t$  = ribbon thickness

$R_1$  = radius of starting cylinder (Figure 2)

If a 1-inch cylindrical melt is assumed, then approximately  $3 \times 10^4$  dynes/cm<sup>2</sup> are required to shape it into a 20-mil-thick ribbon. A thickness of 20 mils has been chosen as a typical thickness of material for device manufacture. Eventually thinner material (8-10 mils) would be desirable. To achieve this, however, increased force and more stability would be required.

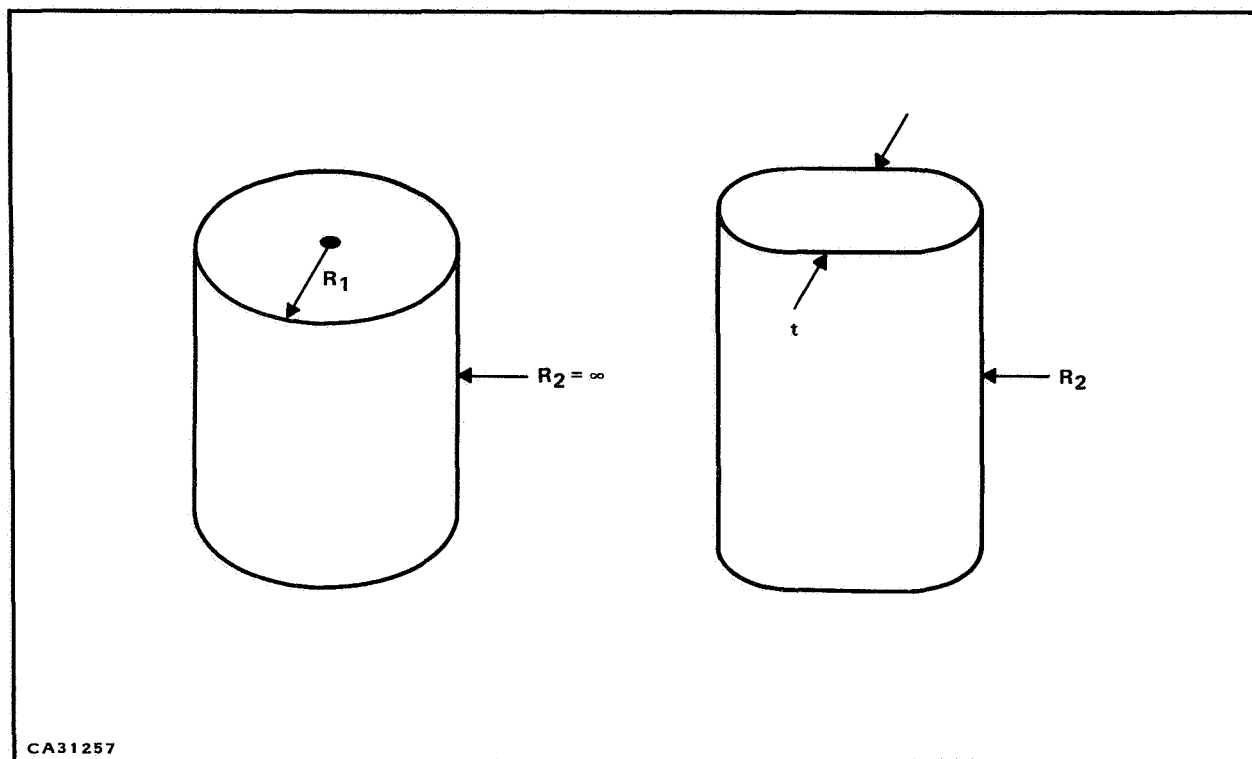


Figure 2. Shapes used for Calculating Surface Pressure

### C. RF Force Density

The force density on the molten silicon may be calculated from solutions to Maxwell's equations for the induced magnetic field and current in the silicon. Using Faraday's equation and Ampere's equation, along with Ohm's law, yields the following relationship for the induced magnetic flux.

$$\nabla^2 \vec{B} = -\sigma \mu \frac{\partial \vec{B}}{\partial t} \quad (1)$$

where

$B$  = magnetic flux

$\sigma$  = conductivity

$\mu$  = permeability

For the particular experimental configuration under consideration, this equation may be reduced to

$$\frac{d^2 \hat{B}_y(z)}{dz^2} - i\omega \sigma \mu \hat{B}_y(z) = 0 \quad (2)$$

where  $e^{i\omega t}$  time dependence has been assumed and we have written

$$\vec{B}(x,y,z,t) = \hat{B}_y(z) e^{i\omega t}$$

The coordinate system is shown in Figure 3. Solving Equation (2), subject to the boundary condition that the tangential magnetic field equals the surface current,  $I_0$ , one obtains

$$B_y(z,t) = -\mu I_0 e^{-\alpha z} e^{i\omega t}$$

where

$$\alpha = \sqrt{i\omega \sigma \mu}$$

The force is derived from  $F = I \times B$ , where  $I$  is given by the curl of  $H$ . The time average force on the surface is given by

$$\frac{F}{A} = \int_0^\infty \frac{1}{2} \operatorname{Re}[\hat{I}_x \hat{B}_y^*] dz$$

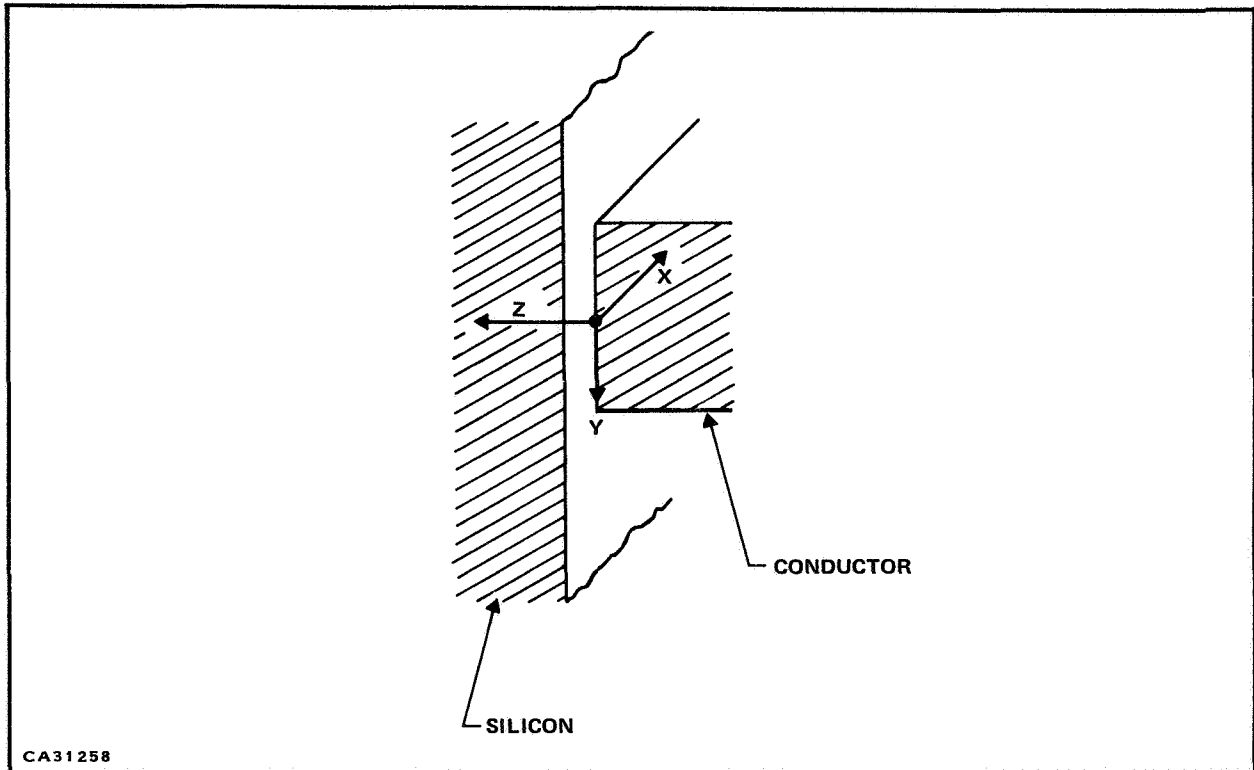


Figure 3. Coordinate System and Orientation of Conductor and Silicon Used in Calculation of Forces of Silicon Ribbon

The surface current required to produce a given pressure is then

$$\frac{F}{A} = \frac{1}{4} \mu_0 I_0^2$$

Since for a 0.020-inch silicon ribbon, the pressure required is approximately  $3 \times 10^4$  dynes/cm<sup>2</sup>, a surface current of  $10^3$  A/cm will be required.

#### D. Force-to-Power Density Ratio

The force density and power density have been calculated for the field-coil silicon ribbon configuration shown in Figure 4. Again, a solution to Maxwell's equation is found which satisfied the boundary conditions:

$$B = \mu_0 I_0 \text{ at } z = -a$$

$$B = \mu_0 I_0 \text{ at } z = a$$

The resultant solution for the magnetic field is:

$$\vec{H} = H_z(x) = \frac{I_0}{(\cos ka)} \cos kx \quad (3)$$

where we have not yet made the quasi-static approximation and where

$$-k^2 = (i\omega\sigma\mu - \omega^2\epsilon\mu)$$

The electric field is derived from

$$\nabla \times \vec{H} = (\sigma + i\omega\epsilon) \vec{E}$$

or

$$\vec{E} = E_y(x) = \frac{1}{(\sigma + i\omega\epsilon)} \frac{\partial H_z(x)}{\partial x}$$

and

$$E_y(x) = \frac{I_0 k \sin kx}{(\sigma + i\omega\epsilon) \cos ka} \quad (4)$$

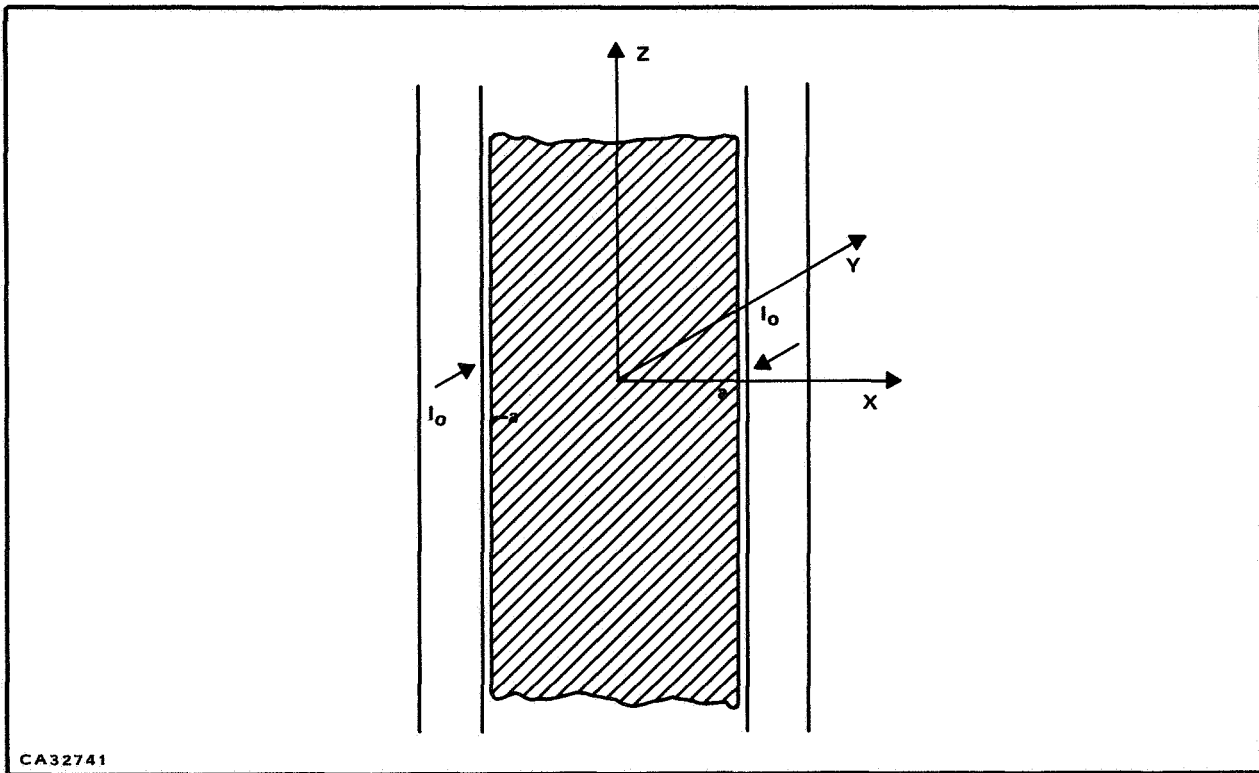


Figure 4. Sample Configuration for Infinite Slab Calculations

The induced current is then given by

$$\vec{J} = \sigma \vec{E}$$

or

$$\vec{J} = J_y(x) = \frac{\sigma I_0 k \sin kx}{(\sigma + i\omega\epsilon) \cos ka}$$

The force on the molten silicon, as well as the power dissipated in the silicon, can be evaluated from the above-derived values of  $\vec{H}$  and  $\vec{E}$  or  $\vec{J}$ . The force density on an element is:

$$\begin{aligned} F &= \frac{1}{2} \text{Re} \left[ \vec{J} \times \vec{B} \right] = \frac{1}{2} \text{Re} \sigma \mu \left[ \vec{E} \times \vec{H} \right] \\ &= \frac{1}{2} \sigma \mu \vec{S} \end{aligned}$$

where

$$\vec{S} = \vec{E} \times \vec{H} \text{ is the Poynting vector}$$

The total force acting on one-half the ribbon is then

$$-F = \frac{1}{2} \sigma \mu \int_0^a (-\vec{S}) dx = \sigma \mu a \langle \vec{S} \rangle \quad (5)$$

where  $\langle \vec{S} \rangle$  is the average value of the Poynting vector. On the other hand, the power dissipated is given by

$$P_d = \int_0^a \nabla \cdot (\vec{E} \times \vec{H}) dx = \int_0^a \nabla \cdot \vec{S} dx$$

The volume integral of the divergence of  $\vec{S}$  is the surface integral of  $\vec{S}$ ; therefore,

$$P_d = -\vec{S}(a) \quad (6)$$

Thus, the ratio of force to power is

$$\frac{-F}{P_d} = \frac{1}{2} \sigma \mu a \frac{\langle S \rangle}{S(a)}$$

Using Equations (3) and (4), both the average value of  $\vec{S}$  and the value of  $\vec{S}$  evaluated at  $a$  can be calculated exactly for either the exact case, where displacement current is included, or the in the quasi-static approximation, where it may be ignored. Since molten silicon is a moderately good conductor, we will assume  $\sigma \gg \epsilon \omega$  and ignore the displacement currents.

Rewriting Equations (3) and (4) in this approximation gives:

$$H_z(x) = \frac{I_0}{\cos ka} \cos kx$$

and

$$E_y(x) = \frac{1}{\sigma} \frac{I_0}{\cos ka} k \sin kx$$

where

$$k^2 \text{ is now } -i \omega \sigma \mu$$

and

$$k = \sqrt{-i \omega \sigma \mu} = (1 - i)^{1/2} \sqrt{\frac{\omega \sigma \mu}{2}}$$

Substituting this value for  $k$  into the expressions for  $\vec{E}$  and  $\vec{H}$  in the Poynting vector gives:

$$\vec{S} = \frac{1}{2} \text{Re} \left[ \vec{E} \times \vec{H}^* \right] \quad (7)$$

$$\vec{S} = S_x(x) = \frac{I_0^2}{2\sigma} \left( \frac{\omega \sigma \mu}{2} \right)^{1/2} \frac{\sin \sqrt{2\omega \sigma \mu} x + \sinh \sqrt{2\omega \sigma \mu} x}{\cos \sqrt{2\omega \sigma \mu} a + \cosh \sqrt{2\omega \sigma \mu} a}$$

The average value of the Poynting vector is then

$$\langle S \rangle = \frac{1}{a} \int_a^0 S_x(x) dx = \frac{I_0^2}{4\sigma a} \left( \frac{\cos \sqrt{2\omega \sigma \mu} a - \cosh \sqrt{2\omega \sigma \mu} a}{\cos \sqrt{2\omega \sigma \mu} a + \cosh \sqrt{2\omega \sigma \mu} a} \right)$$

The value of the Poynting vector at the surface is

$$S_x(a) = \frac{I_0^2}{2\sigma} \left( \frac{\omega \sigma \mu}{2} \right)^{1/2} \frac{\sin \sqrt{2\omega \sigma \mu} a + \sinh \sqrt{2\omega \sigma \mu} a}{\cos \sqrt{2\omega \sigma \mu} a + \cosh \sqrt{2\omega \sigma \mu} a}$$

Thus, the ratio of force to power becomes

$$\frac{F}{P} = - \frac{\sigma \mu}{\sqrt{2\omega \sigma \mu}} \frac{\cos \sqrt{2\omega \sigma \mu} a - \cosh \sqrt{2\omega \sigma \mu} a}{\sin \sqrt{2\omega \sigma \mu} a + \sinh \sqrt{2\omega \sigma \mu} a}$$

This expression has been evaluated for various thicknesses of silicon ribbon (various values of  $a$ ) and plotted as a function of  $\omega$  in Figure 5. It is apparent that, for a given thickness, the F/P ratio is constant in the low-frequency limit. Making the approximation that  $\omega$  is small (expanding and keeping terms to  $\omega^2$  only), the ratio becomes

$$\frac{F}{P} = \sigma\mu \frac{a}{4}$$

This expression has been plotted for silicon in Figure 6 and indicates that the force/power ratio decreases with decreasing  $a$ . Thus, it becomes increasingly difficult to achieve stability in shaping as one goes to thinner ribbon.

In the high-frequency limit, the force-to-power ratio approaches

$$\frac{F}{A} \rightarrow \frac{\mu}{4} I_0^2$$

which is identical to the solution for the semi-infinite space covered with a conduction sheet.

In Figures 7 and 8, the force and power have been plotted as a function of frequency according to Equations (5) and (6), using as the Poynting vector Equation (7).

## 2. PULLER DESIGN

### A. Mechanical System

The initial approach taken on the contract was to fabricate a ribbon puller, based on past experience with crystal growth and on a theoretical treatment of the concept of RF shaping of semiconductors into a ribbon form. The ribbon puller was designed to inductively heat the top of a silicon rod to just below the melting point by using a single-turn RF coil excited by a 1-2 MHz RF generator. A hairpin shaping coil provides sufficient localized energy to melt a stripe on the surface of the feed bar and to shape the melt as it is pulled through the guides. The frequency applied to the shaping guide is determined by the extent to which the RF field is to penetrate the ribbon. For this case, a penetration depth of one-quarter the ribbon thickness was chosen to ensure that the field remains within the silicon, and yet the penetration is sufficiently deep to reduce joule heating.

The mechanical design of the ribbon puller is shown in Figure 9. The upper section of the puller consists of the pull mechanism. This mechanism was designed to allow the continuous pull of ribbon without reseeded. The mechanism consisted of two pair of spring-loaded phenolic rollers which drive either the seed holder or the pulled ribbon, with no interruption in transferring the drive from the seed holder to the ribbon. The center section is the growth chamber. The growth

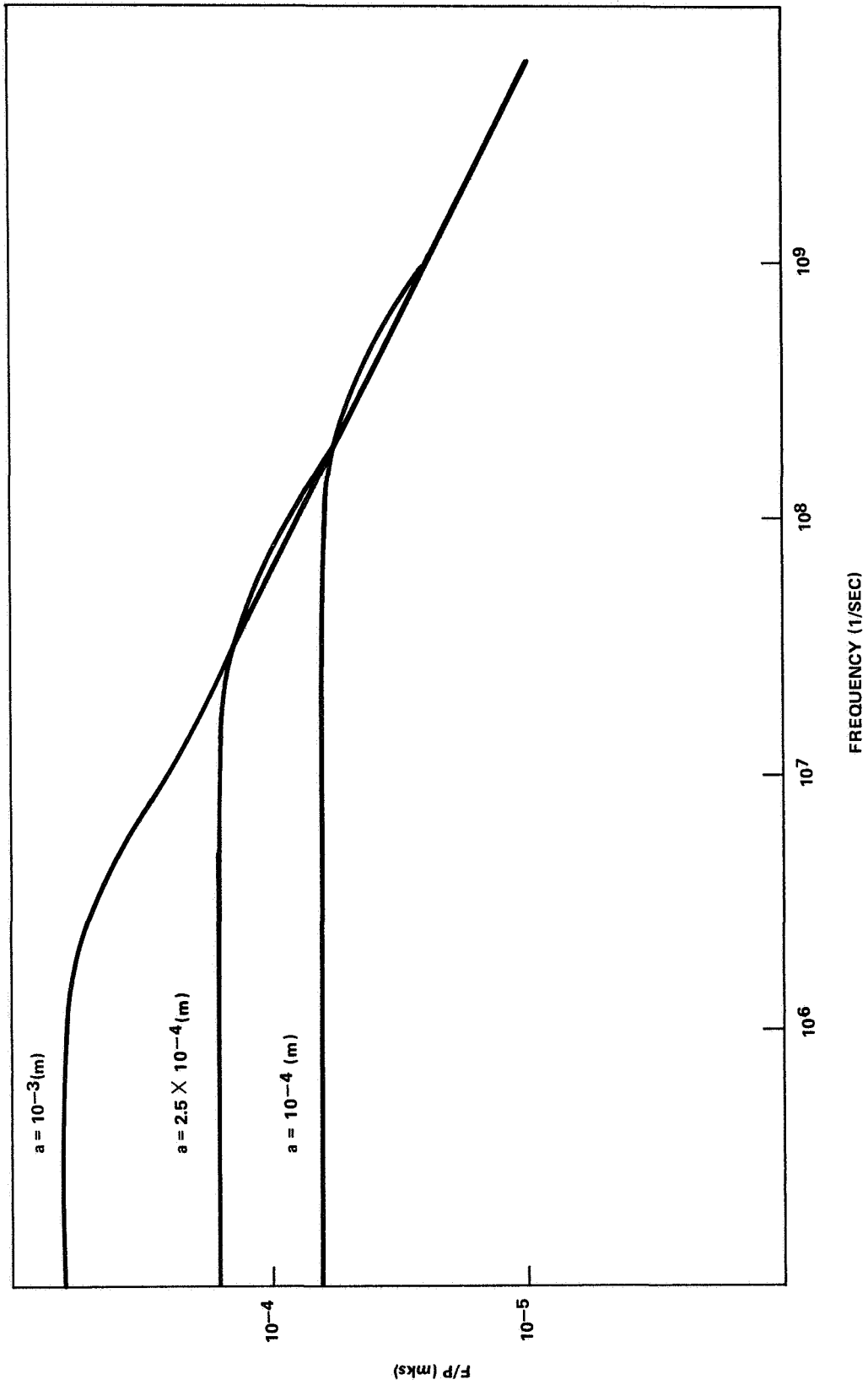


Figure 5. Force-to-Power Ratio for an Infinite Sheet Between Two Conductors

CA32742

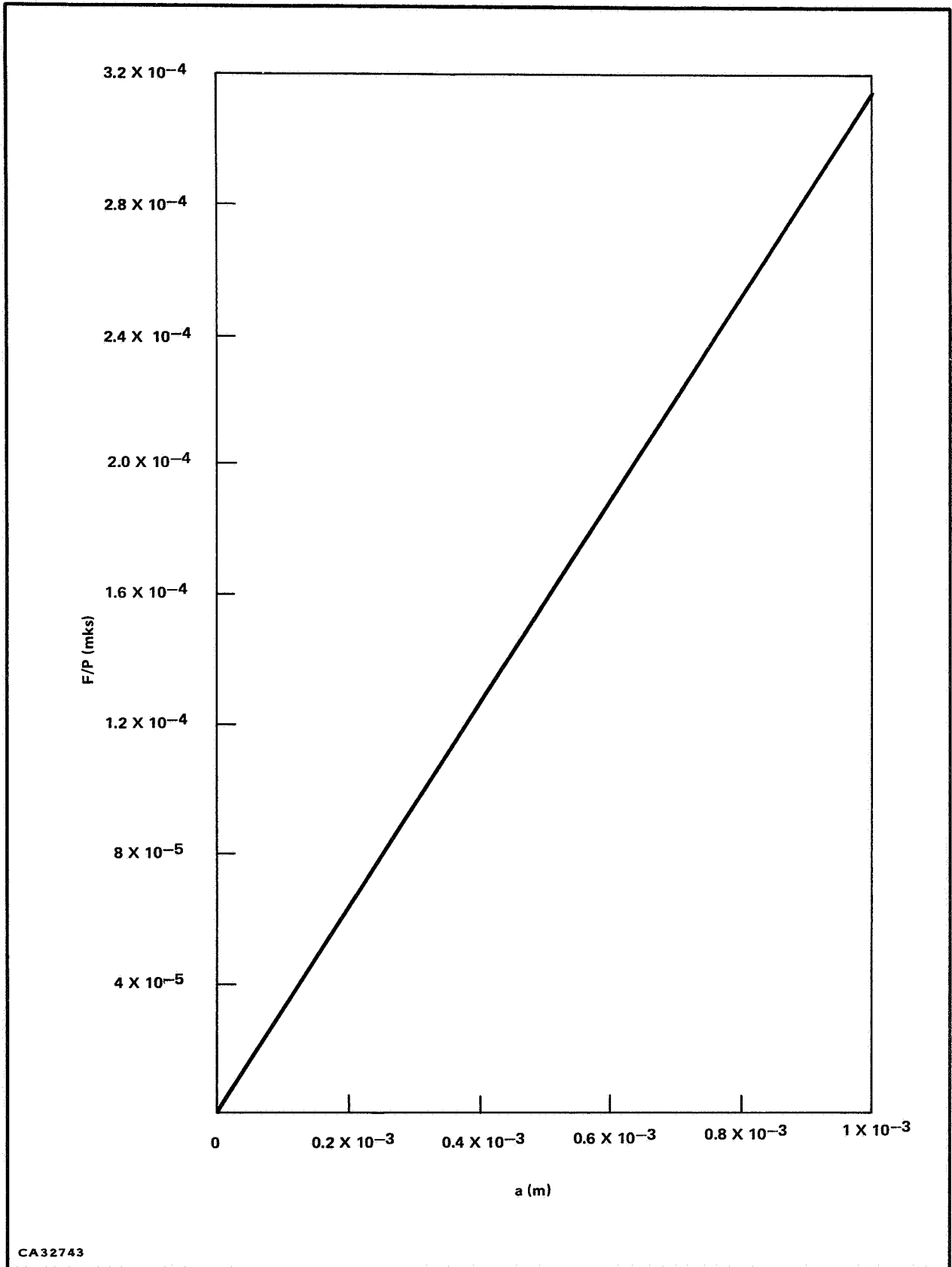
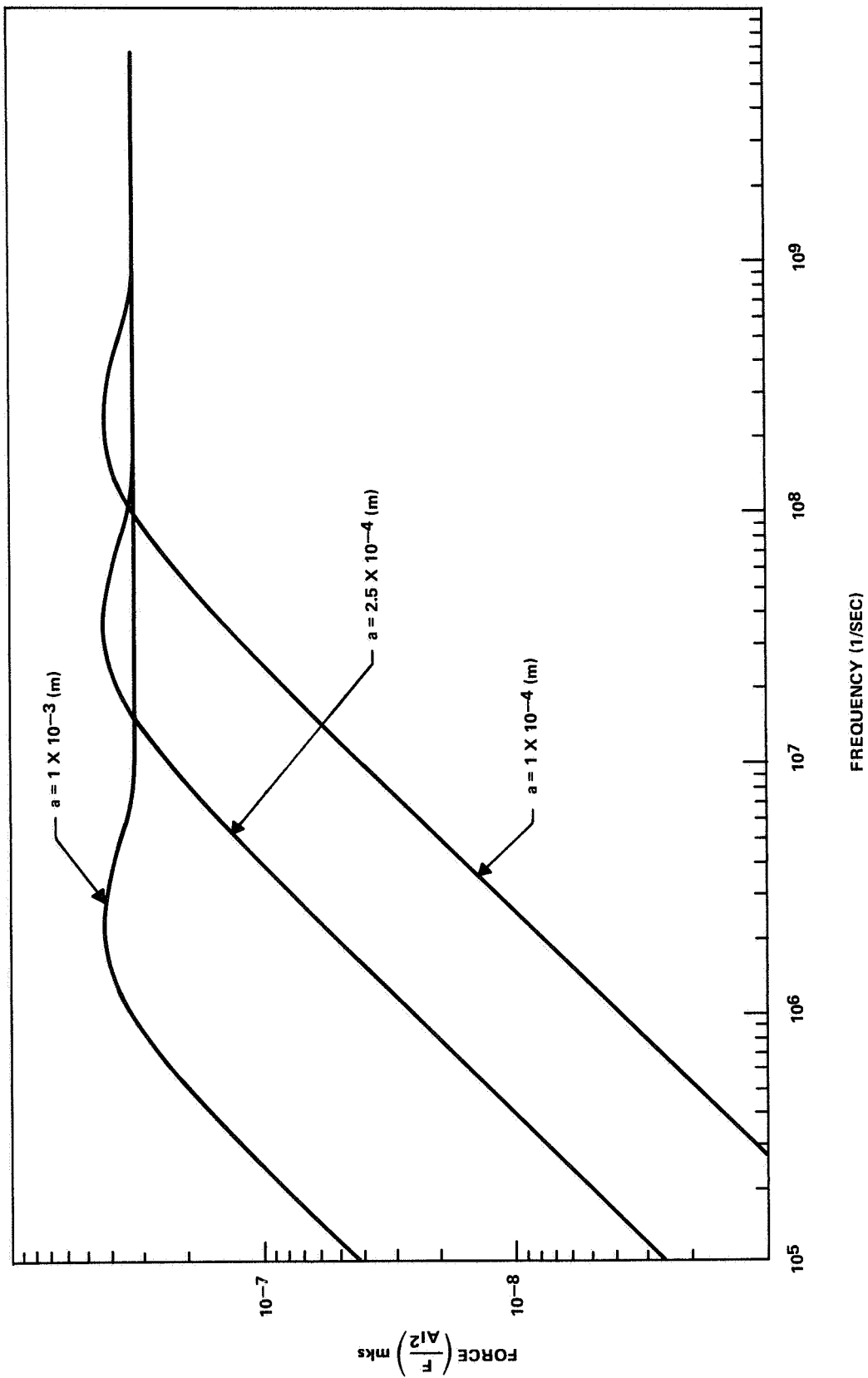


Figure 6. Low-Frequency Approximation of Force-to-Power Ratio as a Function of Ribbon Thickness



CA32744

Figure 7. Force on an Infinite Sheet Between Two Current-Carrying Conductors

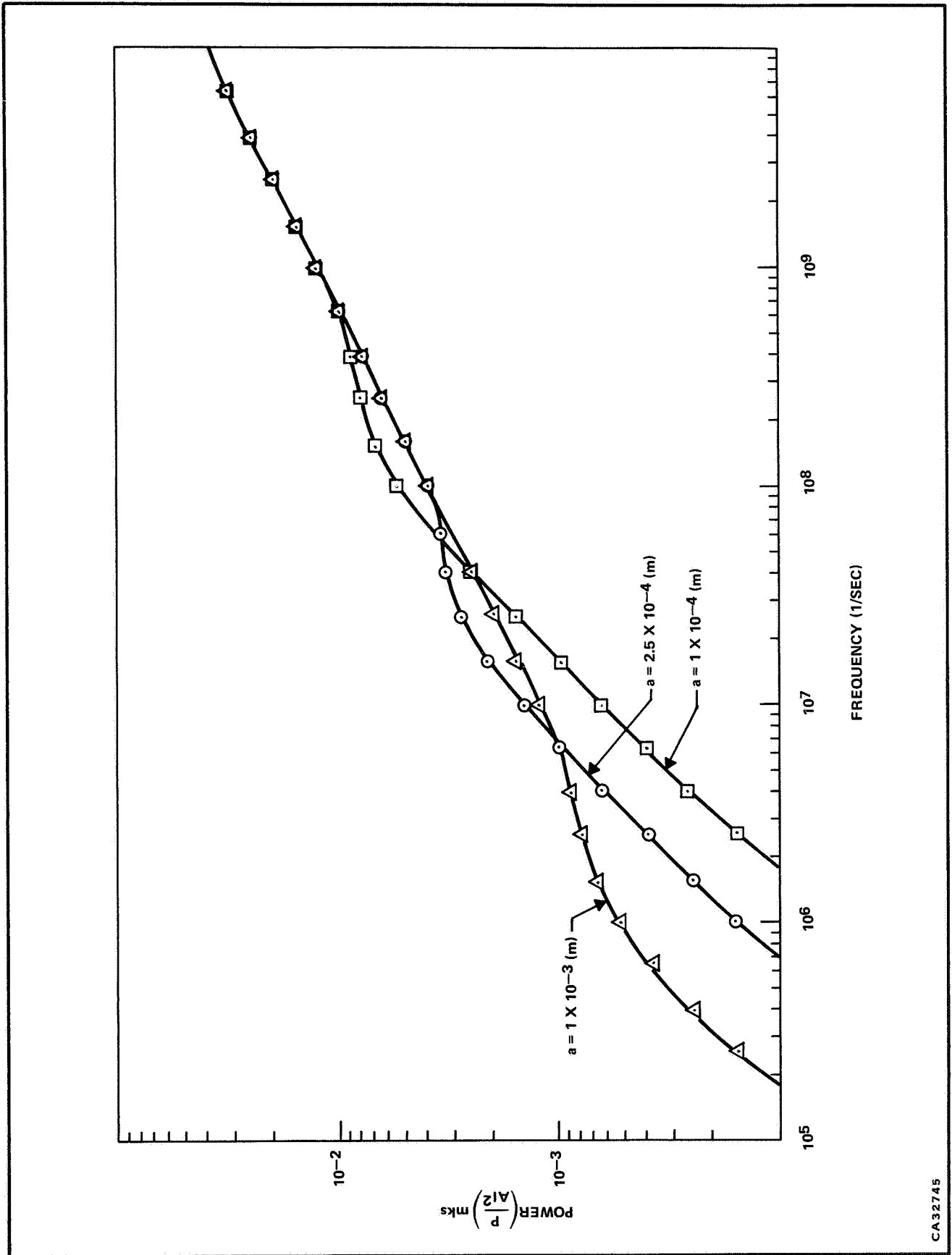


Figure 8. Power Dissipated in an Infinite Sheet Between Two Current-Carrying Conductors

CA32745

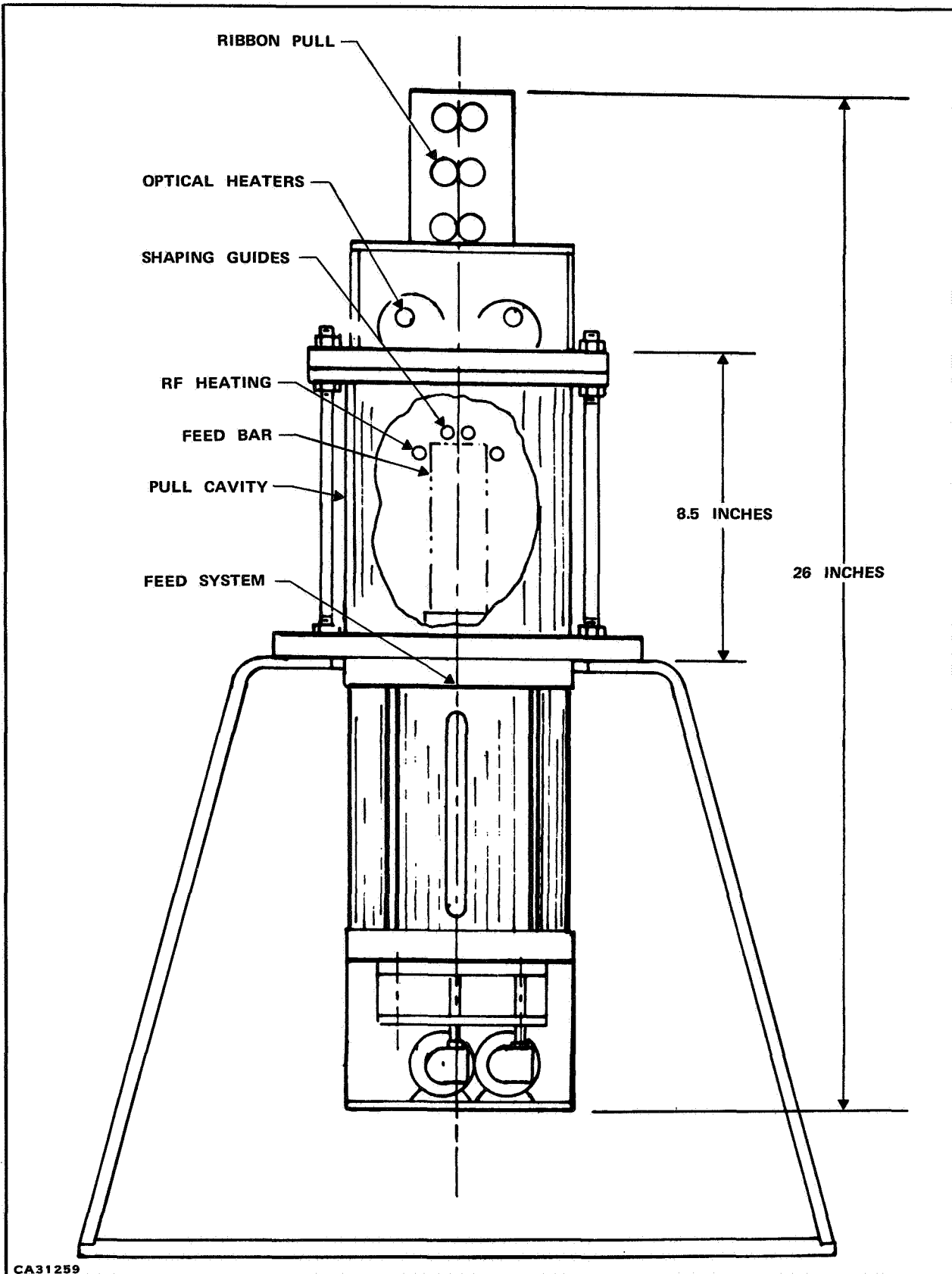


Figure 9. Ribbon Puller System

chamber consists of a Pyrex inner tube with a 5.5-inch inner diameter and a plastic outer tube, with water circulating between the two to provide cooling. Quartz lamps supported above the chamber serve as preheaters to initiate the inductive coupling from the RF sources. In the chamber there is a rotating chuck which can support feed rods of various diameters. The lower section of the puller contains the drive mechanism for the feed bar. It allows rapid or slow elevation of the bar as well as control of the feed bar rotation. A photograph of the ribbon puller is shown in Figure 10, with the various functional regions identified. Drawings of the three sections are included as the Appendix.

## **B. Electrical System**

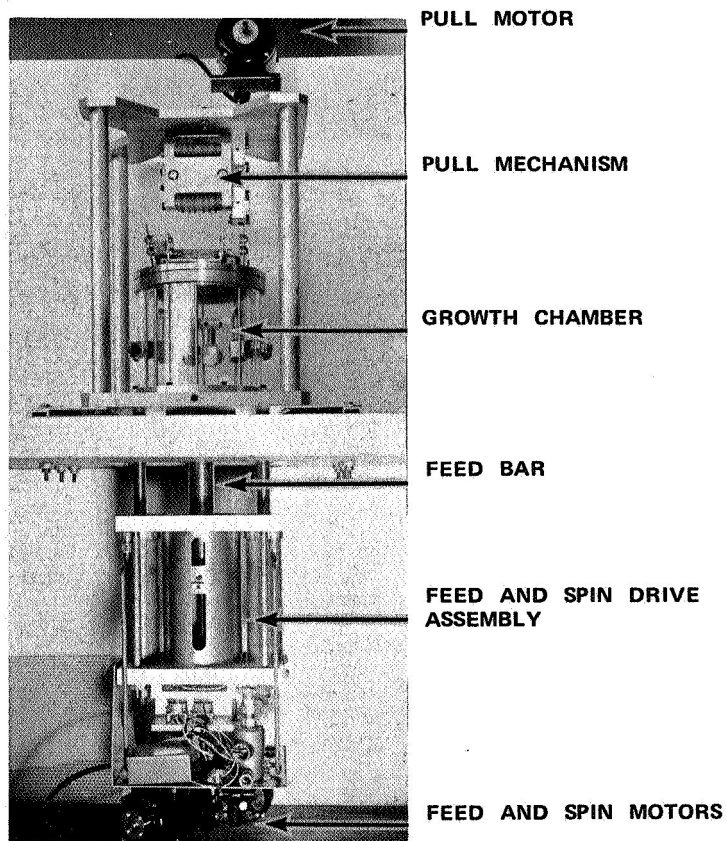
Two coils can be connected to independent RF generators through the walls of the chamber. One of the coils, a large single-turn copper tube is connected to a 2.13 MHz, 15 kW RF generator. The second coil is an especially machined hairpin loop connected to a tunable 15 to 30 MHz, 2.5 kW RF generator. The lower frequency coil is used to form a molten zone at the top of the feed bar, and provides somewhat independent control of the molten zone. The hairpin coil is used to provide the force-fields for shaping the molten silicon.

## **C. Problems**

A number of problems associated with the growth of ribbon using the puller described have been identified. These include gaseous breakdown or arcing, power regulation, and thermal gradients.

The high reactivity of silicon with air causes the formation of an oxide on the surface of molten zone of silicon. This oxide increases the surface rigidity and therefore the forces needed to shape the material. Thus it is necessary to shape the silicon in either a vacuum or in an inert atmosphere. A vacuum chamber is a difficult approach because of the need for a rotating and sliding high-temperature vacuum seal. The choice is then to grow ribbon in an inert atmosphere. Because of the vertical pulling and unsealed growth chamber, argon was used for the inert atmosphere. It is heavier than air and could expel the unwanted gases through the growth slit in the top of the chamber. The argon, however, led to a problem. Its low breakdown voltage prevented the RF generator from operating at full voltage and from delivering sufficient power to the load.

The arcing occurred between the coils or between the coil and the grounded silicon bar. The arcing between the bar and coil was eliminated by isolating the bar and the seed from the puller by using quartz supports. The arcing between the coils was eliminated by using quartz spacers between the regions of large potential difference.



CA31260

Figure 10. Silicon Ribbon Puller Without Control Panel

A second problem encountered was that the power supply of the 2.5 kW Lepel generator to be used for shaping was not filtered. The unfiltered power supply produced a 120-cycle amplitude-modulated RF current in the shaping guides. The outputs of the power supply and oscillator in the unfiltered state are shown in Figures 11(a) and 11(b). It has been demonstrated in floating zone reactors that if the RF signal in the load coils is amplitude-modulated, then the electromagnetic-induced forces are also amplitude-modulated and this modulation produces a vibration in the melt. This vibration is due to the modulation of the high frequency forces, and not to the low frequency induced forces. In our system, this vibration would prevent the growth of dislocation-free single crystal silicon and also cause undulation in the surface topography. A filter was connected to the output with the resultant RF waveform shown in Figure 11(c).

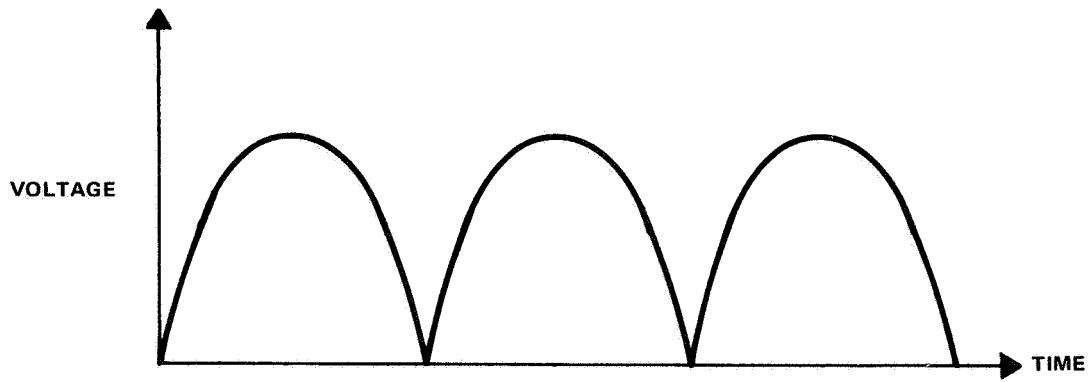
### 3. FORCE MEASUREMENTS

#### A. Introduction

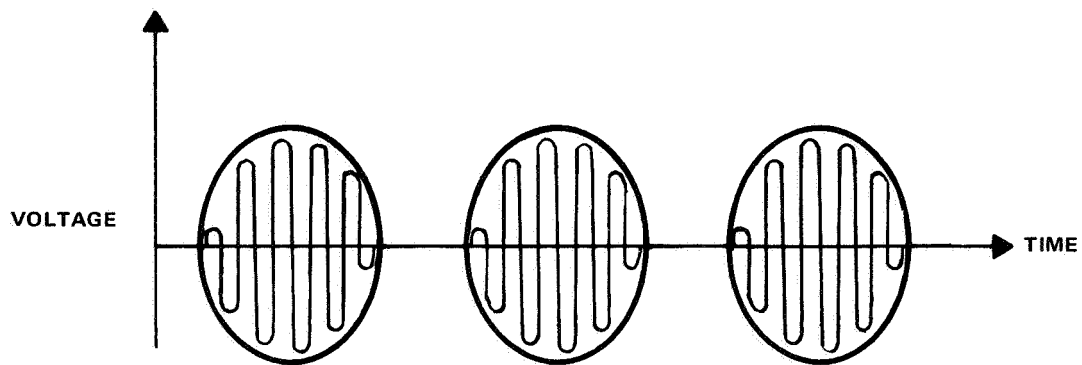
A lack of literature, theoretical and especially experimental, characterizing forces induced in molten materials by RF fields has required an investigation of the basics of RF forces. The single article which was found to describe shaping of molten semiconductors, was entirely theoretical with

#### B. Method

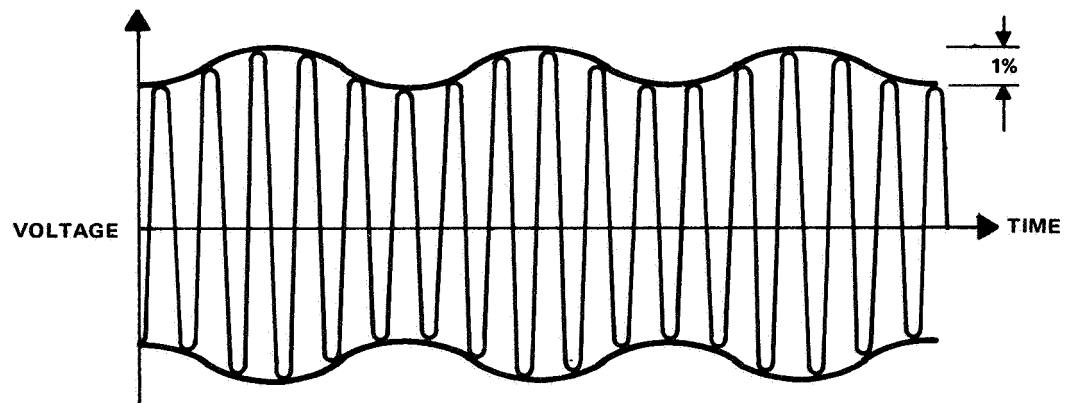
A simple arrangement has been devised for the measurement of axial and radial forces induced in molten silicon by currents flowing in a simple single or multiturn coil. The experimental arrangement has been depicted in Figure 12. A quartz bucket of known diameter and containing a fixed amount of silicon is fastened to a torsion balance by a thin quartz filament. The torsion balance consisted of a balance beam supported by a molybdenum wire connected to a wheel calibrated in degrees, which could be rotated to maintain the position of the beam where desired. Either a 20-mil or a 10-mil molybdenum wire was used as the torsion spring. The spring constant of the 20-mil wire was 1.33 mg/deg, while the spring constant of the 10-mil molybdenum wire was 0.108 mg/deg. The torsion balance was used in the horizontal configuration to measure the axial forces, as illustrated in Figure 12 and pictured in Figure 13. The radial forces were measured with the torsion balance in the vertical configuration, as illustrated in Figure 14. The bucket is suspended in the field of the RF coil, its position being adjusted by the torsion spring of the balance. When the RF field is turned on or changed, the bucket comes to a new equilibrium position. The spring can then be adjusted to return the bucket to its original position. The change in force exerted by the torsion spring is equivalent to the force exerted on the silicon by the RF fields. By setting the bucket at various positions with the RF field off, it is possible to get a force map for the given physical configuration of the coils and bucket.



(a) OUTPUT OF UNREGULATED POWER SUPPLY



(b) OUTPUT OF OSCILLATOR WHEN PLATES BIASED BY UNREGULATED POWER SUPPLY



(c) DESIRED OUTPUT OF RF OSCILLATOR

CA30102

Figure 11. Power Supply and Oscillator Outputs

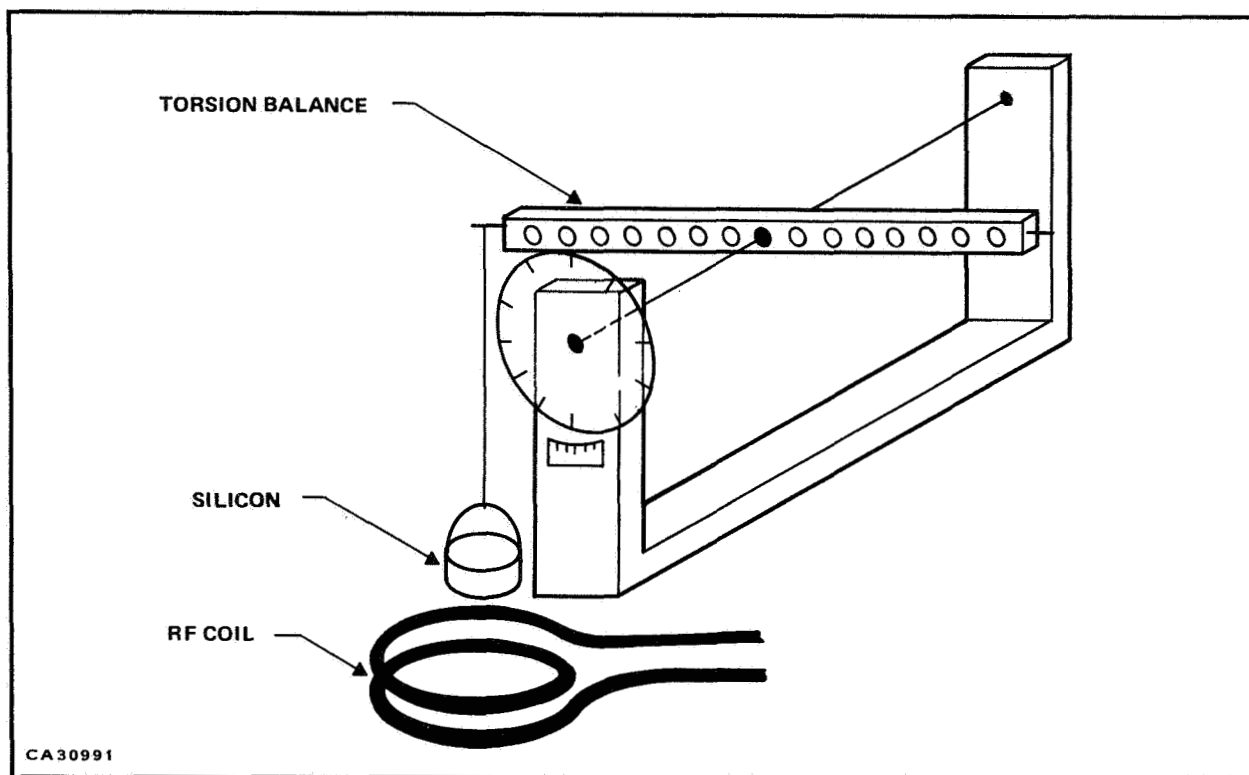


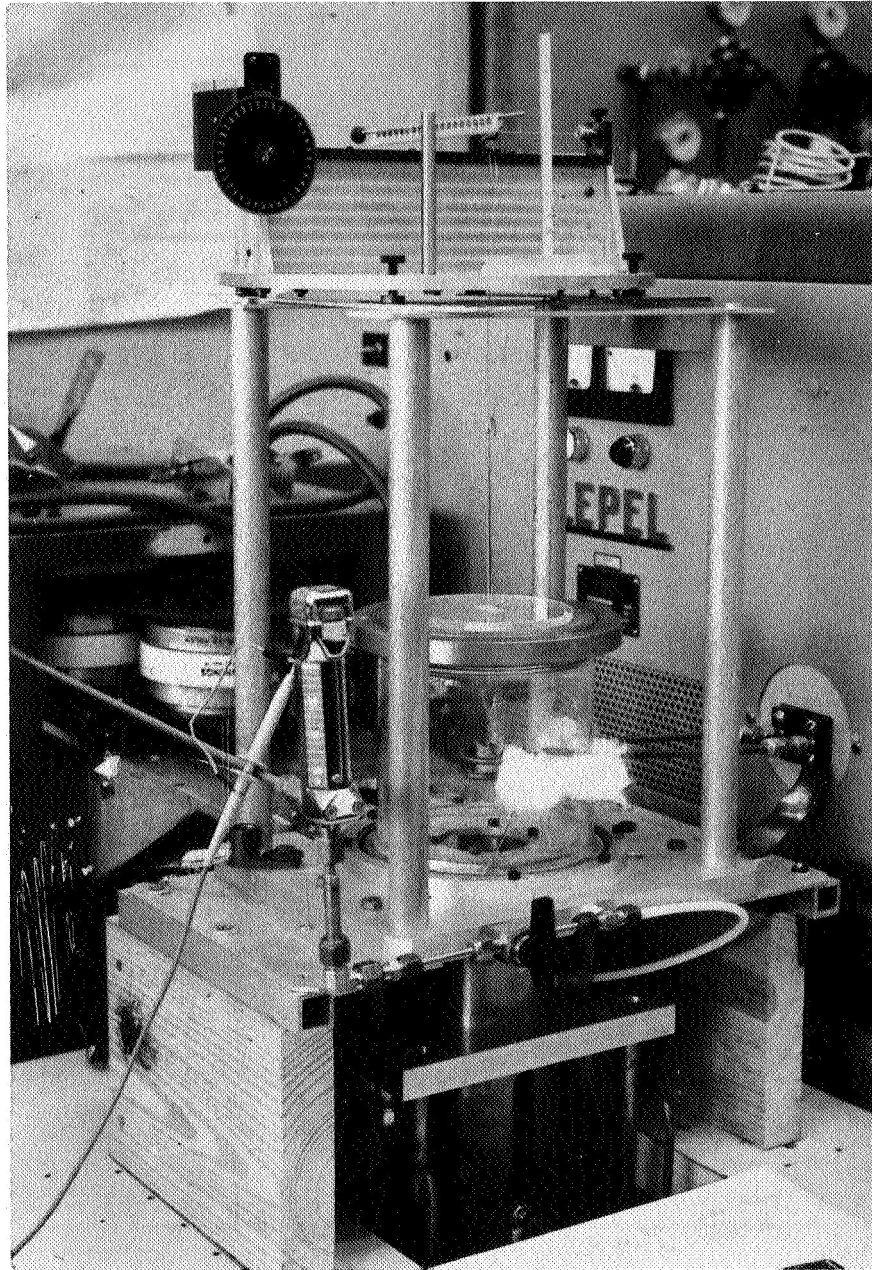
Figure 12. Torsion Balance for Measuring Axial Force

As described earlier, the relationship between the induction heating of the sample and the force density acting on the molten zone is critical. A primary variable which allows some control of the relationship between the heating and force density is the frequency. It was decided to characterize the forces at more than one frequency. Operation at several frequencies however, leads to a number of impedance matching problems. For a given coil and sample configuration, both the resistive and reactive components of the load impedance change as the frequency is changed. The initial experiments at various frequencies were performed with a constant power delivered to the tank circuit by the oscillator. This did not ensure constant power delivered to the load because of the impedance mismatch between the load coil and the RF tank circuit.

As an example of the change in impedance as a function of frequency, the magnitude and phase angle of the impedance of the two-turn coils were measured at 13.75 MHz and 20 MHz, the two frequencies at which data were taken. The results are:

13.75 MHz	33 $\angle$ 88° ohms
20.0 MHz	45 $\angle$ 90° ohms

These impedances were measured with no load in the coil. The presence of a load only slightly alters the impedance.



CA32746

Figure 13. Photograph of Torsion Balance for Measuring Axial Force

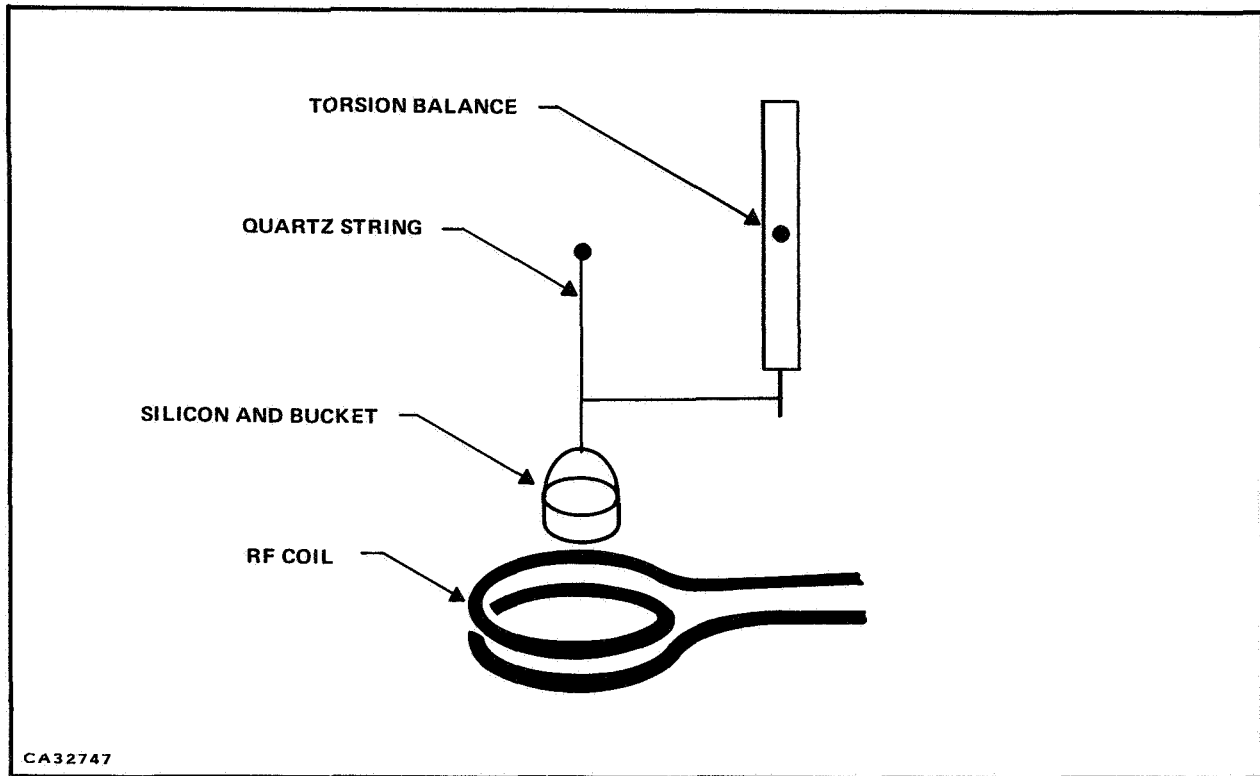
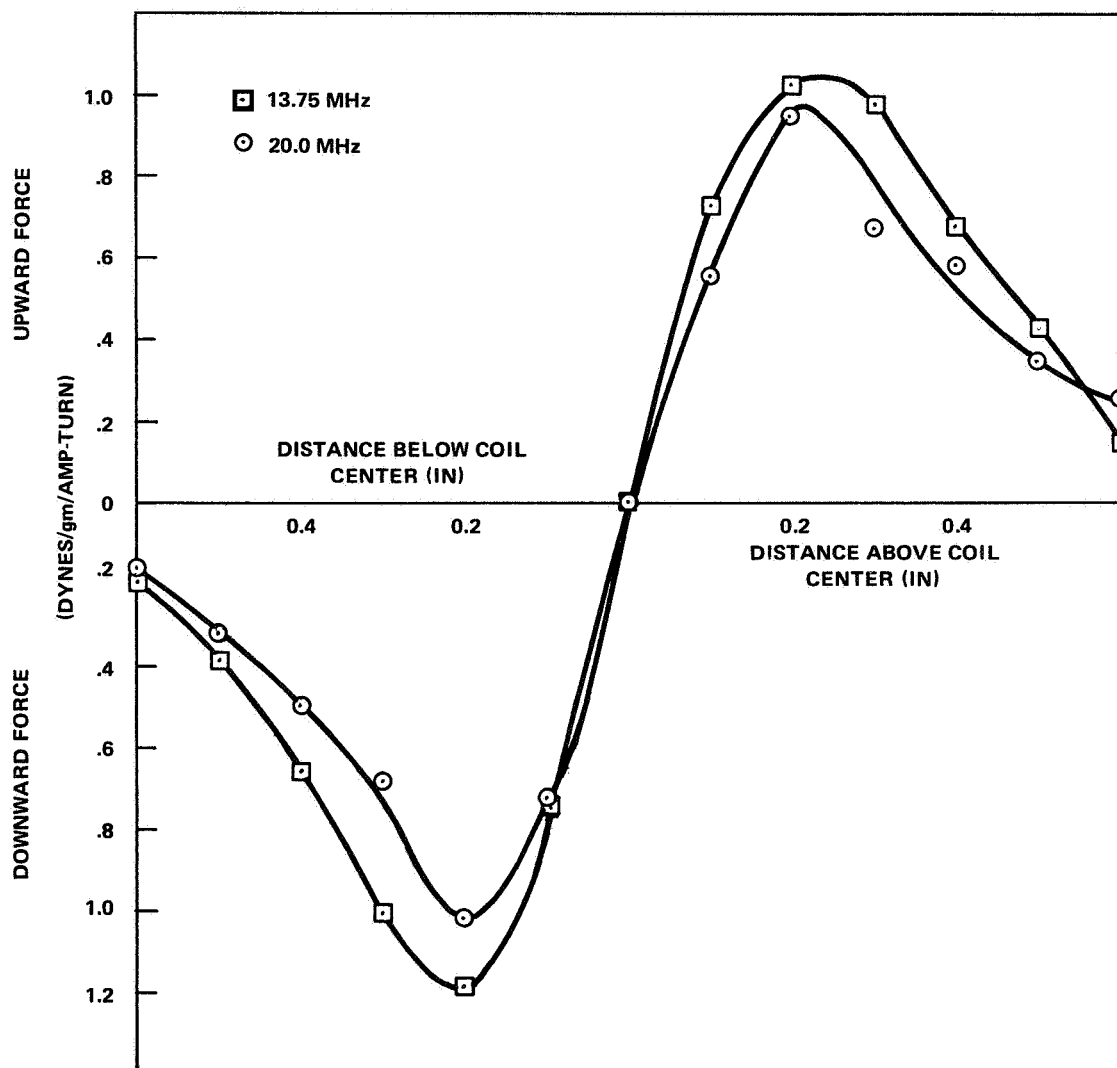


Figure 14. Torsion Balance for Measuring Radial Force

In order to normalize the forces produced for a given power to the load, a method of measuring the RF current flowing in the load coil was implemented. A known low-impedance circuit is inserted in series with the load coil and the RF voltage drop measured with a high-frequency oscilloscope. From the value of the impedance and the voltage drop, the current was determined. The impedance of the series circuit was  $2.3 \angle 75^\circ$  ohms at 13.75 MHz and  $3.3 \angle 88^\circ$  ohms at 20.0 MHz.

### C. Axial Forces

The axial forces on a molten silicon cylinder were measured for drive frequencies of 13.75 MHz and 20.0 MHz. The load coil was a double-turn coil formed with 3/16-inch O.D. copper tubing with a coil I.D. of 0.75 inch. A 3.076-gm silicon charge was suspended in a quartz bucket with a 0.5-inch I.D. The length of the molten zone in this instance was 0.45-inch. The resultant force acting on the molten silicon as a function of axial position for frequencies of 13.25 MHz and 20 MHz is plotted in Figure 15. The force has been normalized to dynes/gram/amp-turn to eliminate the problem of change in impedance when the frequency changes. Within the experimental error, the forces on the molten silicon at 13.75 MHz and 20 MHz are identical. When the center of the melt is in the plane of the coil, there is no net force on the molten zone. The force reaches a maximum when the entire melt is just outside the plane of coil, and as the silicon is moved farther from the plane of the coil, the forces decrease.



CA31091

Figure 15. Measured Axial Forces on Molten Silicon

An explanation of the forces plotted in Figure 15 may be obtained by referring to Figure 9. The forces are proportional to the field strength, which decrease with distance from the center of the coil. Above the coil plane, the forces active on the molten silicon are upward, while below the coil plane the forces acting on the molten silicon are downward. When the molten zone has equal volumes of material above and below the plane of the coil, the upward and downward forces are equal and the resultant force is zero. This is just the case of Figure 16(a). In Figure 16(b), the situation is depicted where a greater portion of the melt is above the coil than below. There is therefore a net upward force equivalent to a melt of length  $L_1$  located above the coil by an amount  $L_2$ . The maximum force is achieved when the entire melt is just above the plane of the coil, as shown in Figure 16(c). As the melt is moved away from the coil, the force begins to decrease since the field decreases with distance from the coil.

#### D. Radial Forces

Radial forces in the plane of the coil have also been measured. These data were taken using a 2-MHz RF generator. The force measurements were made prior to the impedance characterization of the RF induction heating coils. The circulating current was not measured and the normalized forces could not be determined. The radial dependence was measured however, and the results are presented in Figure 17. The results are for 3 grams of silicon suspended in a quartz bucket on the radius of a two-turn coplanar coil with an I.D. of 2.125 inches. The force decreases from the edge of the coil, reaching zero net force at the center of the coil.

A second set of radial force measurements was made using the 2.5-kW generator turned at 13.75 MHz and 20.0 MHz. A 2.10-inch, inner-diameter coil was used. The current was calculated from the voltage measured across a known impedance. The normalized force as a function of radial position for the two frequencies is shown in Figure 18.

### 4. RIBBON GROWTH

#### A. Introduction

During the period of the contract, numerous attempts were made to grow silicon in a rectangular form through the use of RF forces. The first attempts were made using the puller as initially conceived, that is, with a 2-MHz melt-forming coil and a 15-MHz melt-shaping coil. Subsequently, a single coil was used, due to the difficulties encountered with two coils. The procedures which were followed and the changes which were made in the system are described in the following subsections.

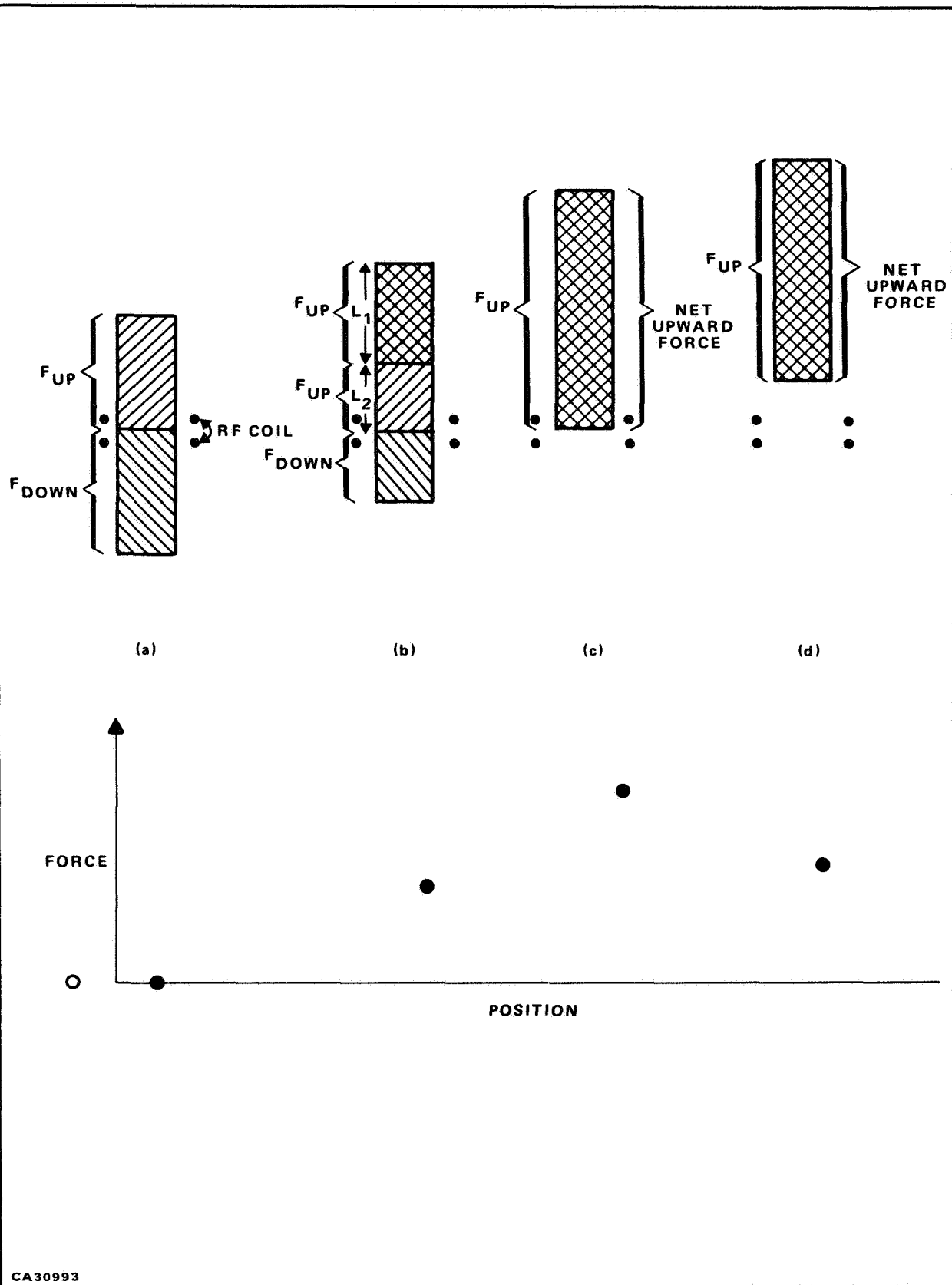


Figure 16. Force as a Function of Melt Position Relative to RF Coil

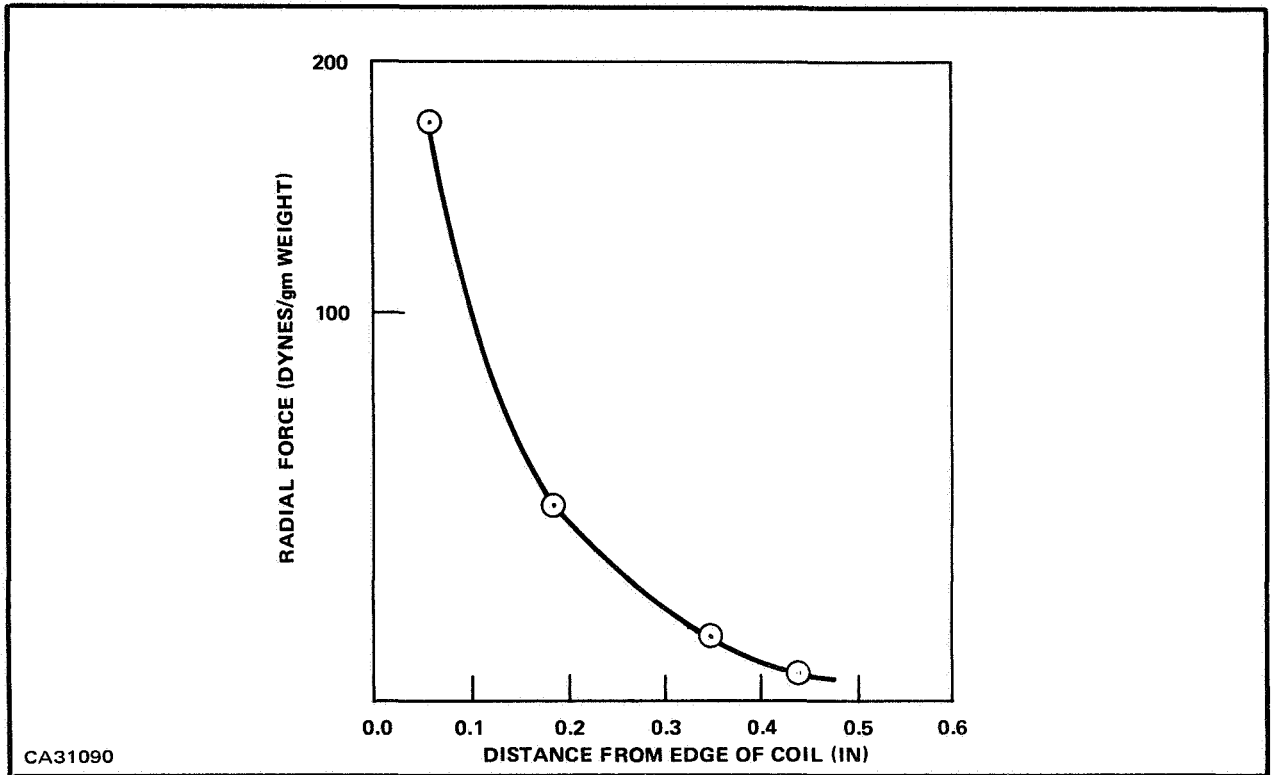


Figure 17 Measured Radial Dependence

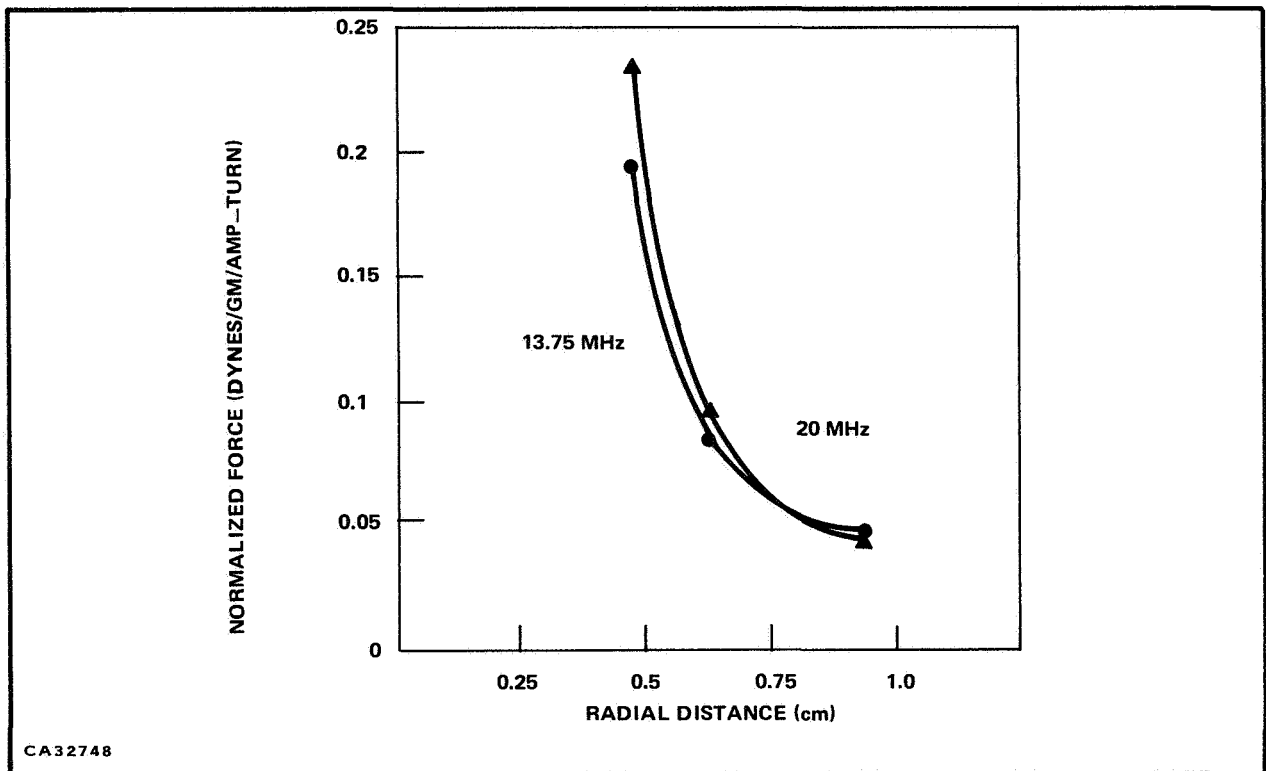


Figure 18. Normalized Radial Force versus Distance from Coil Edge

## B. Two-Coil System

In the two-coil system, the two coils were arranged as shown in Figure 19. The lower coil (A) was driven by a 2-MHz, 15-kW RF generator and was intended to form a molten zone on the top surface of the silicon feed bar. The upper coil (RF shaping guide) was machined to close tolerances and was connected to a 8- to 30-MHz, 2.5 kW, variable-frequency RF generator. The high fields developed at the edges of the shaping guide were intended as the solidifying form of the silicon. The bar and coils were enclosed in a cold-walled Pyrex chamber through which an inert gas was flowing. Argon was chosen because it is denser than air and could, therefore, expel the unwanted gases through the orifice on the top plate, through which the seed and ribbon were pulled.

The initial attempts to pull ribbon were performed with the configuration described above. However, before a molten zone could be formed on the top of the feed bar, the argon ionized and gaseous discharge occurred between the coil and the base plane of the growth chamber. This problem was eliminated by center tapping the low-frequency coil and grounding it to the base plane as shown in Figure 20. Grounding the coil in such a manner effectively halved the voltage developed across the load coil. This was sufficient to eliminate the arcing to the base plate ground.

Elimination of the breakdown path from the high potential side of the coil to the base plate introduced a new low-resistance path for gaseous discharge. Again, as the power to the low-frequency coil was increased, discharging occurred. In this instance, the breakdown occurred between either side of the input to the low-frequency coil and the feed bar. This presented a serious problem, introducing a discharge path through the feed bar to the mounting chuck, which was at ground potential. This problem was overcome by using a thin-wall quartz tube 1 to 2 inches long as a standoff. The tube was clamped to the rotating chuck and the feed bar was wired to the tube. With the standoff in place and the coil center tapped, all arcing was eliminated and a molten zone could be formed on the top of the feed bar with the 2-MHz generator.

After the molten zone was formed, the high-frequency generator was turned on and a 15-MHz signal applied to the shaping coil. The close proximity of the melting and shaping load coils to one another caused a second problem. The feedback coil from the tank circuit to the oscillator tube of the low-frequency oscillator had a self-resonant frequency of approximately 15 MHz. As the power to the shaping coil was increased, high-frequency currents in the feedback coil of the generator developed and it overheated. The solution to this problem was to operate the shaping oscillator at a frequency at which the feedback choke did not resonate. Fortunately, the Q of the choke was sufficiently high that operation at either 14 MHz or 16 MHz was possible.

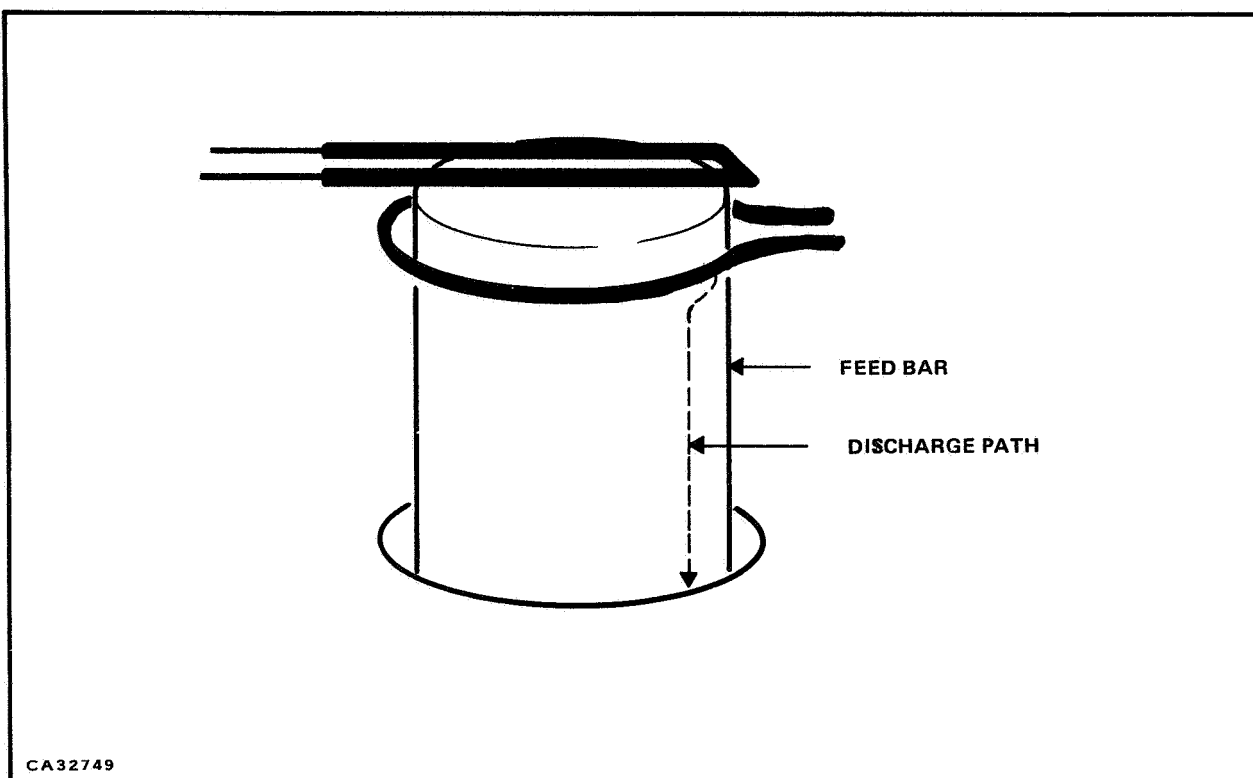


Figure 19. Dual-Frequency Coil Arrangement

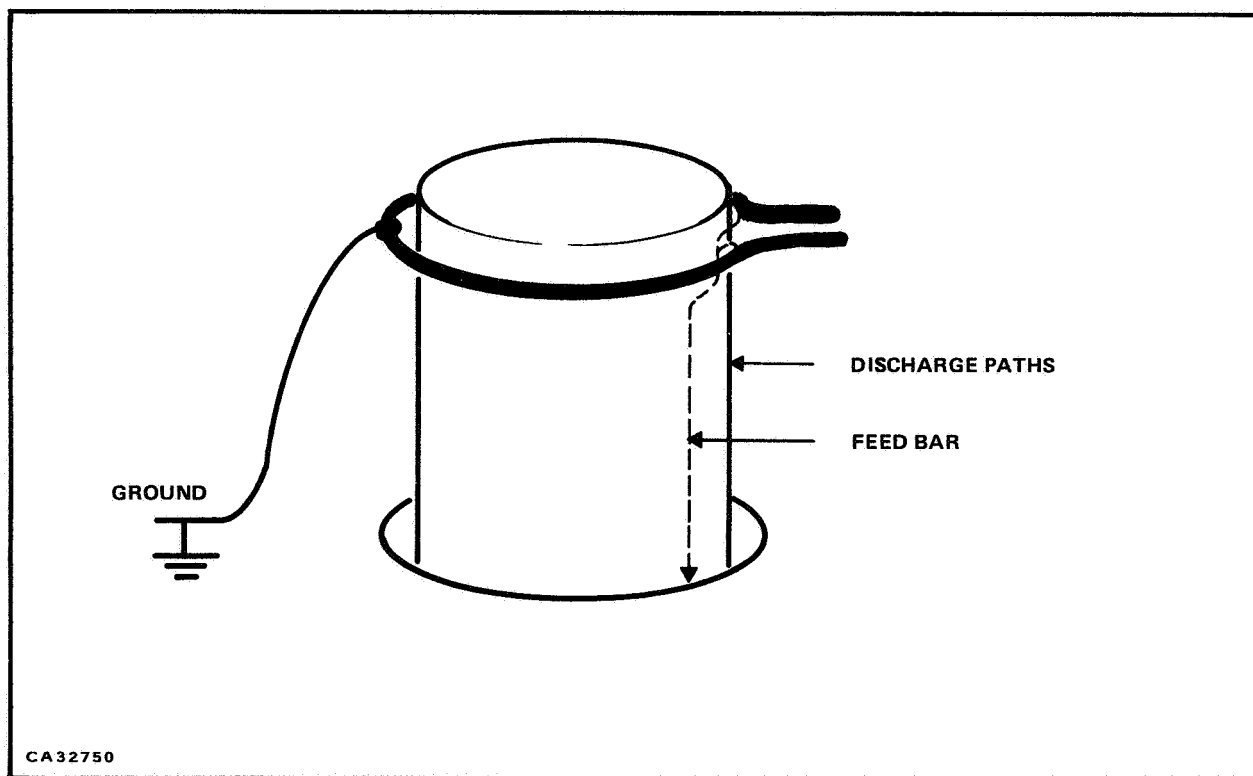


Figure 20. Center-Tapped Power Coil

With the molten zone formed and the shaping-oscillator operating, the initial attempt to pull a ribbon was made. A 20 X 400 X 1000-mil seed was cut from a silicon rod. Anticipating arcing from the shaping coil to the seed, the seed was isolated from the pull rod by a quartz plate. Arcing was less of a problem with the shaping coil since the applied potential of the high-frequency RF generator was less than that of the low-frequency generator. No attempt was made to lower the voltage by use of a transformer since high currents would then be required to deliver sufficient RF power and the resistive losses in the coils would be too high.

The seed was lowered into the force field of the shaping coils and one of two things happened:

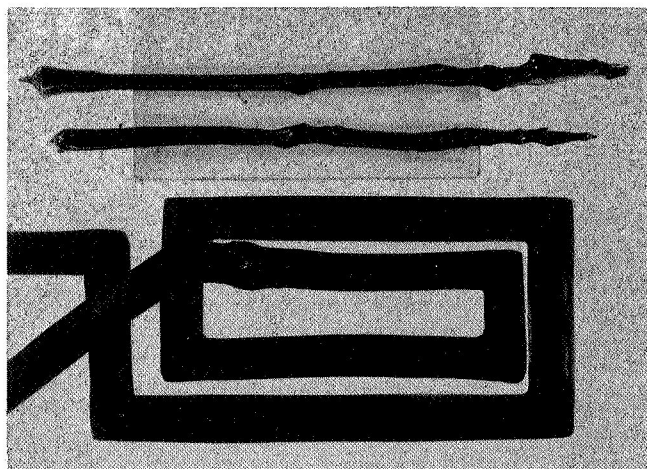
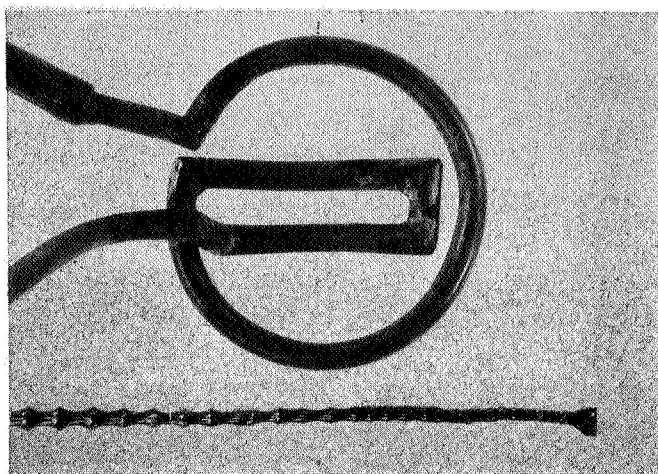
- 1) The seed oscillated between the shaping guides, eventually striking one of the guides and remaining in contact.
- 2) The seed oscillated between the shaping guides, coming to rest between them.

In the event that item (2) occurred, the seed could be lowered into the molten zone, which was rotating slowly to prevent dropoff. Dropoff is the spilling of molten silicon from the molten zone down the side of the solid bar. It occurs because of the asymmetrical melting of the zone, primarily due to the asymmetrical heating coil.

The seed was held just above the melt for 5 to 10 minutes prior to "seeding in" to raise its temperature substantially. The seed was then dipped into the melt. As the seed entered the melt, the molten silicon would pile up against it because of the large planar shape. This resulted in a torque on the seed which moved it into the shaping guides. Numerous attempts were made to pull ribbon using the configuration described above. In all cases, the seed was either pushed into the shaping coils by the melt, or, on pulling, the seed separated from the melt. Because of the inherent difficulties with the two-coil system, such as arcing, oscillation, and melt formation, it was decided to use a single, complexly wound coil for both melting and shaping the silicon, as described in the following subsection.

### C. Single-Coil, Complex-Wound System

Since numerous difficulties were encountered using independent generators for both forming the molten zone and shaping the silicon, a single coil which was to form the molten zone and provide the shaping forces was fabricated. The design of these coils is shown in Figure 21. This coil was connected to the 2-MHz, 15-kW generator, a 0.75-inch diameter feed bar was clamped to the chuck, and a 40 mil X 250 mil X 4-inch seed was fastened to the pull rod. Initial attempts to pull ribbon using this configuration resulted in a crystal with a circular cross section. The feed bar was then raised to within 100 mils of the rectangular guide and further attempts to shape the silicon were made. The first attempt produced a stem which was not circularly symmetric. The ratio of the width to thickness for the stem varied from 1.1 to 1.2, the largest ratio for the largest-diameter



CA31261

Figure 21. Shaped Material Coils

material. This would be consistent with RF shaping. As the stem became larger, it would be closer to the coil and the shaping forces would increase. Another attempt was made to grow shaped material. This time, the power was reduced to bring the silicon as close as possible to the rectangular portion of the coil. In this instance, the width-to-thickness ratio varied from 1.33 at a diameter of 0.11 inch to 1.63 at a diameter of 0.218 inch. Again, the maximum ratio was reached for the largest diameter. Further attempts to reduce the power to bring the stem even closer to the rectangular shaping coil resulted in the freezing of the molten zone because of insufficient induction heating.

The circular-rectangular coil was modified with the distance between the rectangular turn reduced from 0.4 inch to 0.25 inch. The intent was to bring the coil closer to the silicon. Again, the problem of oscillator power controlling both the induction heating and RF forces prevented the growth of flat-form silicon ribbon.

## 5. SOLIDIFICATION IN A MAGNETIC FIELD

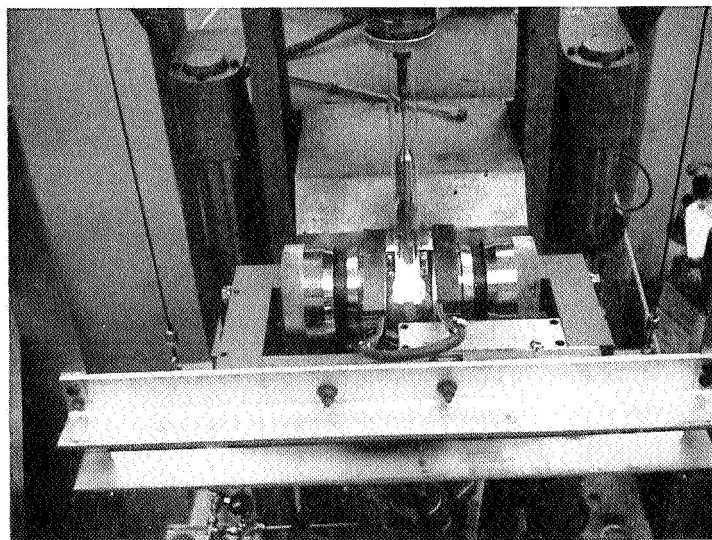
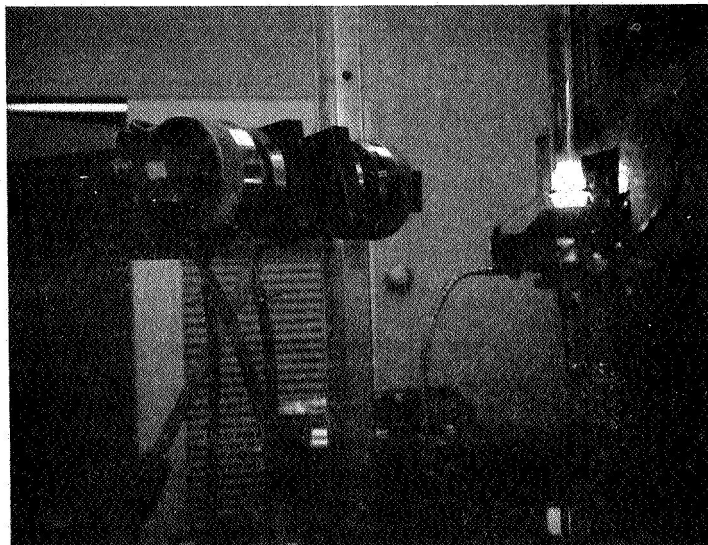
Included in the first task was the growth of the ribbon in the presence of a static magnetic field. The growth in the field was to be accompanied by passing a dc through the silicon to achieve levitation by the Lorentz force field. A preparatory experiment was performed to determine the influence of a magnetic field on crystal growth.

A high resistivity polycrystalline rod prepared from vacuum float zone was solidified into single crystal form in an on-off type of magnetic field. The growth of the single crystal was beside the float-zone process with the Dash technique to grow the crystal dislocation-free. A crystal approximately 0.900 inch in diameter and 13 inches in length was grown.

The object was to introduce a magnetic field after about 3.5 inches of crystal were grown [the (x.l) ratio should be such that segregation from solidification has reached steady state] The field was to be left on for about 2 inches of crystal growth and then removed.

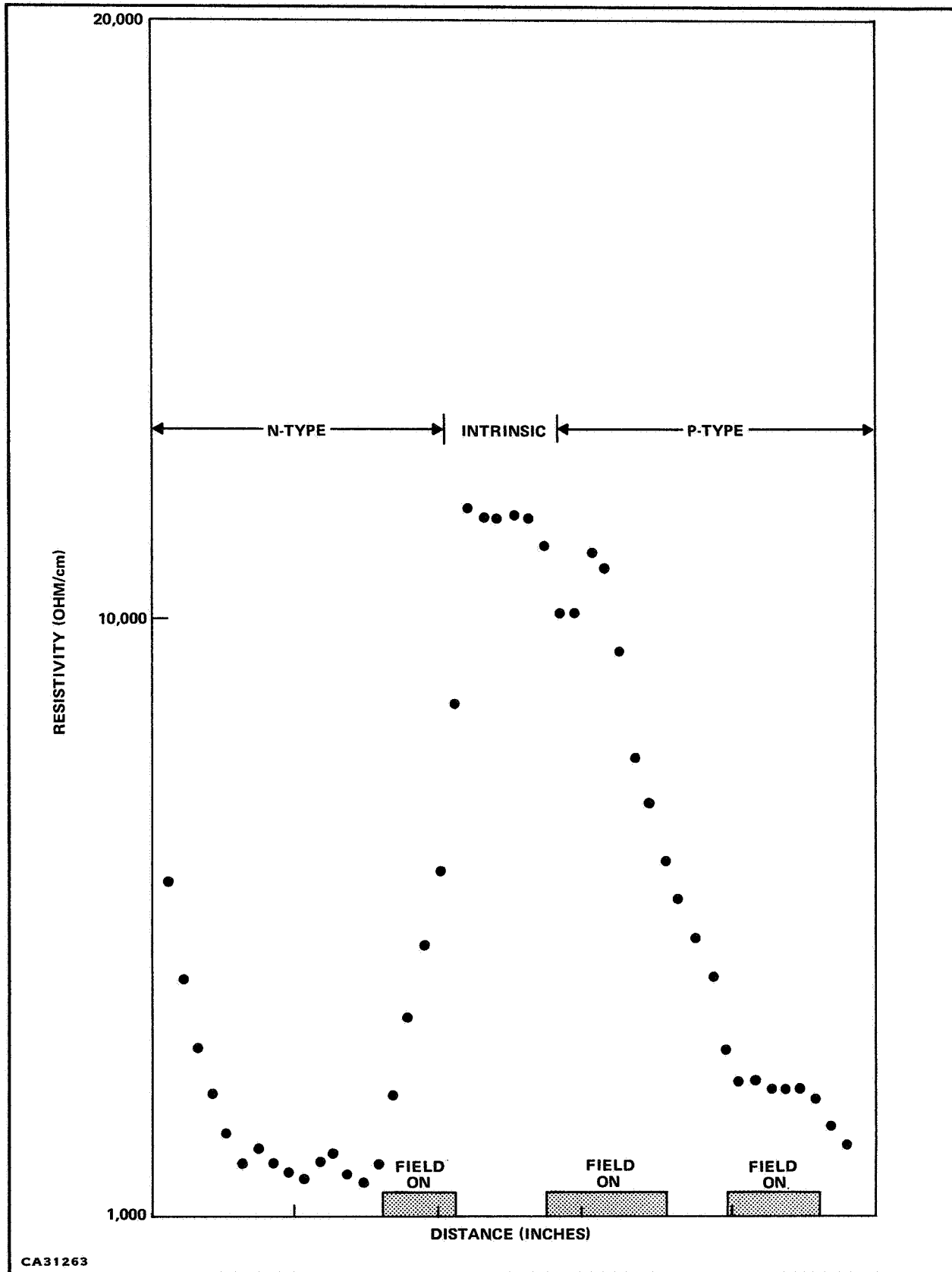
The magnetic field was produced by a permanent magnet and the experimental setup is illustrated in Figure 22.

After the magnet was removed, the crystal was permitted to grow for about 2 inches without a magnetic field. The magnetic field was then reintroduced for another 2 inches and then removed. This on-off sequence of the magnetic field was repeated once again. The crystal grew dislocation-free down to the bottom 2 inches, indicating that the magnetic field did not affect crystalline perfection as determined by the absence or presence of dislocations. The change in resistivity and type is shown in Figure 23. The limited characterization which has been accomplished makes it difficult to correlate the presence of the magnetic field with the electrical properties, and further experiments are needed.



CA31262

**Figure 22. Dislocation-Free Silicon Growth in the Presence of a Magnetic Field**



**APPENDIX**

**DETAILS OF THE RIBBON PULLER**

ITEM	QTY	DWG SIZE	PART NUMBER	DESCRIPTION
1	1	C	96101	GEAR HOUSING
2	2		FH-11-03-03-8-011	GENERAL TIME CLUTCH
3	2			GEAR MODIFIED BOSTON Y6432
4	2			GEAR BOSTON Y64160
5	1	A	96102-1	SHAFT
6	8		96103	STAND OFF
7	1	A	96102-2	SHAFT
8	8		4-40 X 1"	SCKT HD 4-40 X 1"
9	1	C	96104	DRIVE SUPPORT PLATE
10				
11	1	A	96105	LIFT NUT
12	1	B	96106	WATER SUPPLY GLAND
13	4	A	96107	SUPPORT RODS
14	1	C	96108	SPINDLE ASSEMBLY
15	1	A	96109	TOP SEAL
16	1	C	96110	TOP GUIDE PLATE
17	1	A	96111	SPIN DRIVE GEAR
18	2	A	96113	CYLINDER CAP LOWER
19	4			BEARINGS BOSTON 1606 DC
20	1	B	96112	LIFT SCREW
21	2			JAM NUTS 3/8-24
22	3			QUAD RINGS 1-1/2 ID X 1/8 NOM SECTION
23	1			QUAD RING 2" ID X 1/8 NOM SECTION
24	1	B	96114	SUPPORT TUBE
25	2	B	96115	PISTON AND ROD ASSEMBLY
26	3			"O" RING 1-1/2 ID X 1-3/4 OD I/E SECTION
27	2		96116	CYLINDER CAP UPPER
28	2			BUSHING BOSTON 3/4 X 1-1/8 X 1-1/4 B-1218-10
29	2		96117	CYLINDER

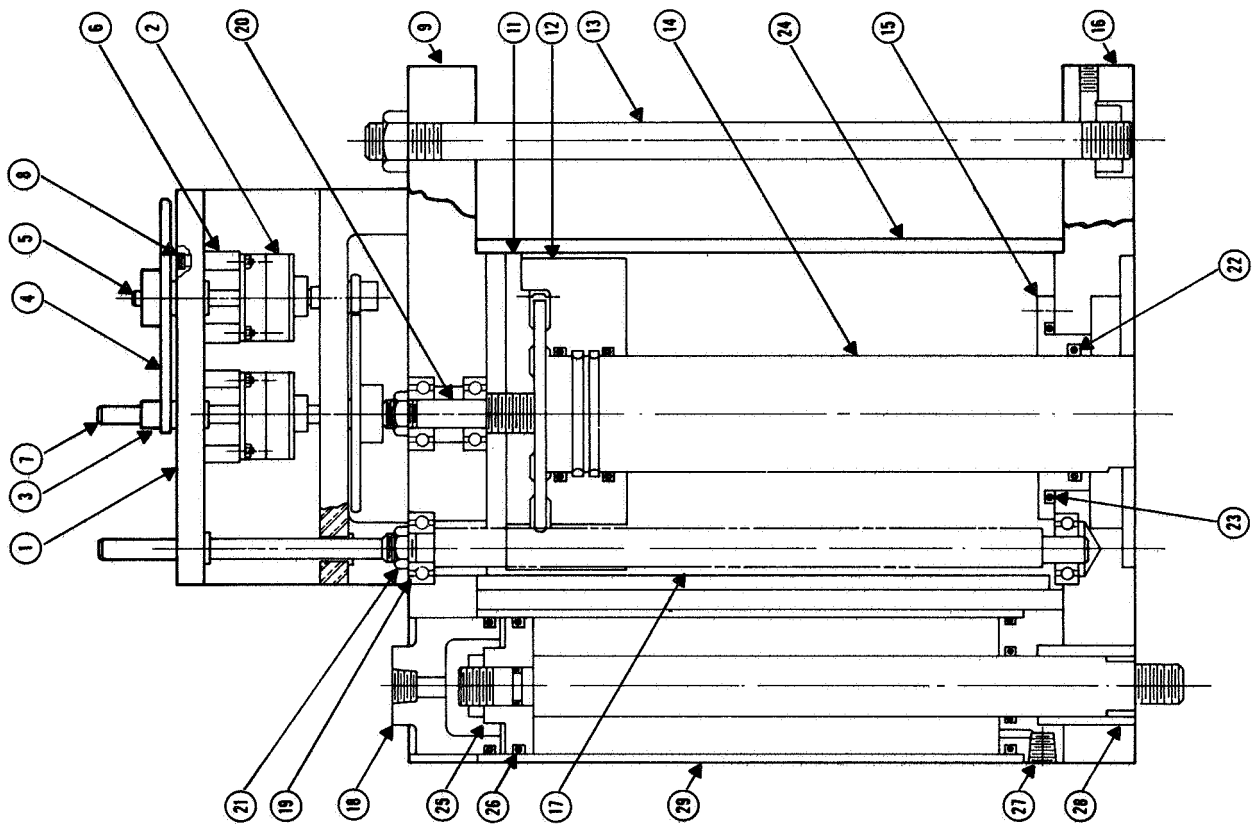


Figure A-1. Drive Assembly - Ribbon Puller

CA31264

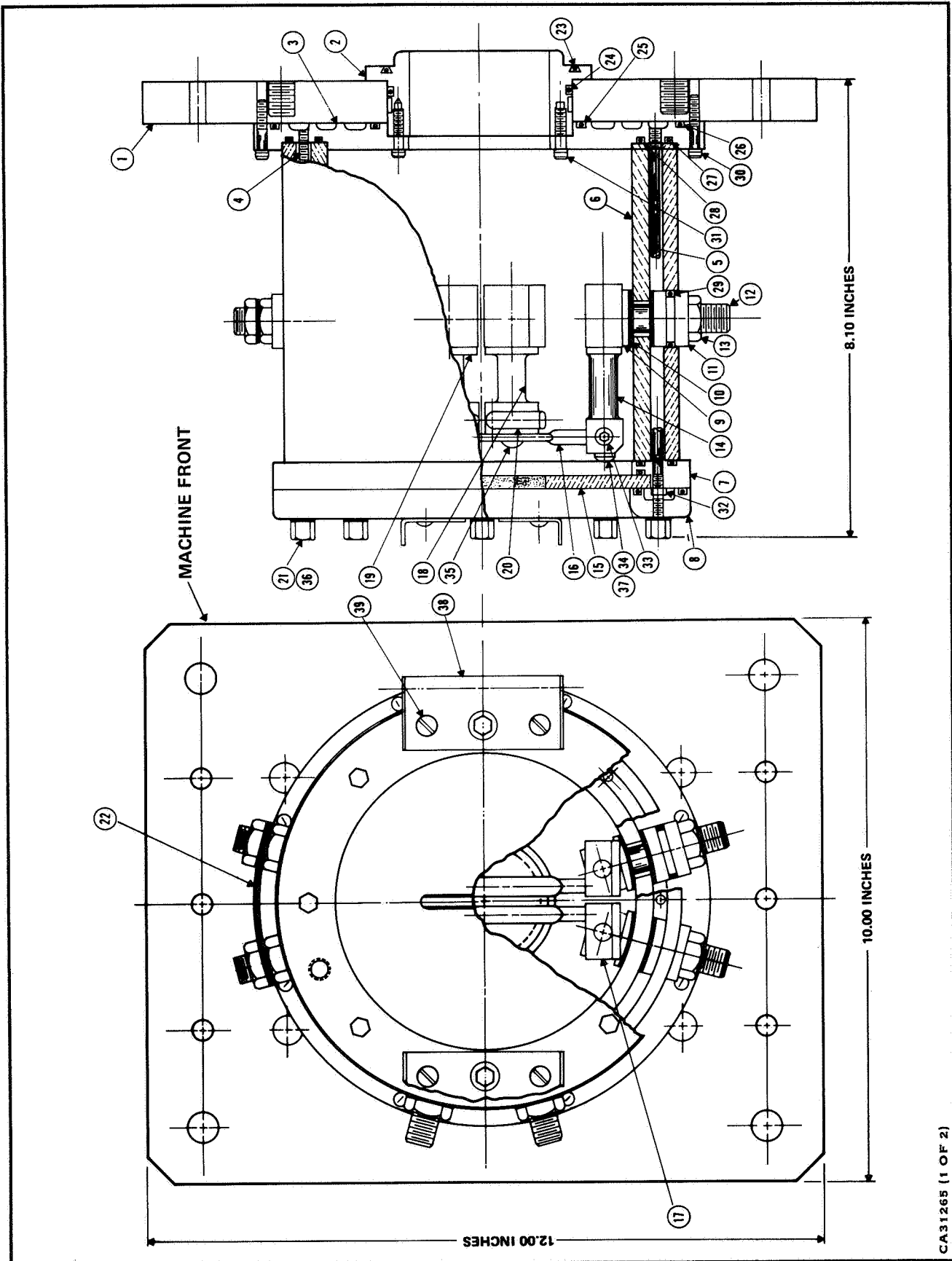


Figure A-2. Cavity Assembly - Ribbon Puller (Sheet 1 of 2)

ITEM	QTY	DWG SIZE	PART NUMBER	DESCRIPTION
1	1	C	96301-A	CAVITY BASE
2	1	B	96302-A	LOWER SEAL
3	1	C	96303-A	LOWER SEAL PLATE
4	8	A	96304-A	DRAW BOLT
5	1	B	96305-A	PULLER WALL PYREX
6	1	B	96306-A	COOLER WALL PLEXIGLASS
7	1	B	96307-A	TOP SEAL RING
8	1	B	96308-A	TOP RING
9	6	A	96309-A	TUBE SADDLE INSIDE
10	12	A	96310-A	SADDLE SEAL
11	6	A	96311-A	TUBE SADDLE OUTSIDE
12	6	A	96312-A	RF FEED THRU
13	8			HEXAGON NOT BRASS JAM 1/2"-28
14	2	B	96313A-1	RF GUIDE HOLDERS
15	1	B	96314-A	SUPPORT PLATE QUARTZ
16	2	A	96315-A	RF SHAPING GUIDE
17	2	B	96313A-2	RF GUIDE HOLDER
18	1	B	96313A-3	RF GUIDE HOLDER
19	1	B	96313A-4	RF GUIDE HOLDER
20	1	A	96316-A	RF HEATER
21	8	A		CAP NUTS 8-32
22	2		96318-A	SHORTING STRAP
23	1			"O" RING 3 1/4" ID X 1/8" SECTION
24	1			"O" RING 3" ID X 1/8" SECTION
25	1			"O" RING 3 1/2" ID X 1/8" SECTION
26	2			"O" RING 7" ID X 1/8" SECTION
27	2			"O" RING 6 1/2" ID X 1/8" SECTION
28	4			"O" RING 5 1/2" ID X 1/8" SECTION VITON
29	6			"O" RING 1" OD X 1/8" SECTION
30	8			SCKT HD CAP SCREW 10-32 X 1" LONG
31	6			SCKT HD CAP SCREW 10-32 X 1 1/2" LONG
32	8			HEXAGON NUTS 8-32 BRASS
33	6			1/16" SCKT HD PIPE PLUGS
34	4			10-32 X 2 1/2" PAN HD SCREW
35	2			10-32 X 2 1/4" PAN HD SCREW
36	8			SERIES 800-030-8 PARKER LOCK-O-SEAL
37	6			SERIES 800-030-1/4" PARKER LOCK-O-SEAL
38	2		96319-A	PIVOT BRACKET
39	4	A		10-32 X 1/4" LONG PAN HD SCREWS

NOTE 1  
NOTE 1

CA31265 (2 OF 2)

Figure A-2. Cavity Assembly – Ribbon Puller (Sheet 2 of 2)

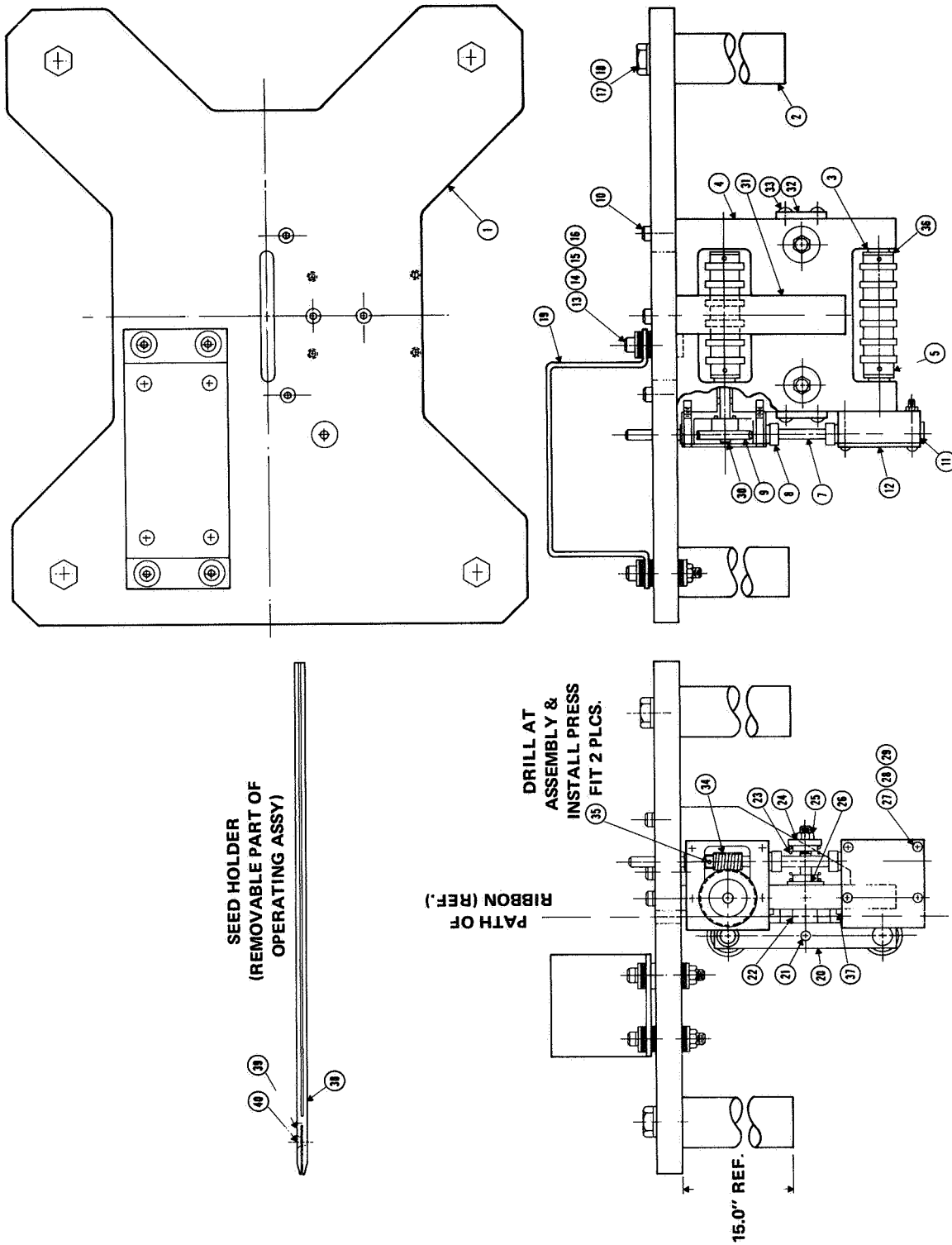


Figure A-3. Pull Mechanism – Ribbon Puller (Sheet 1 of 2)

CA31266(1-2)

ITEM	QTY	DWG SIZE	PART NUMBER	DESCRIPTION
1	1	C	96601	TOP PLATE
2	4	A	96602	SUPPORT POST
3	20	A		BUSHING BOSTON FLANGED FB35-3
4	1	B	96603	3/16 ID X 5/16 OD X 3/8 LG
5	4	A	96604	SUPPORT HOUSING
6				ROLLERS RIBBON DRIVE
7	1	A	96605-1	3/16 DIA WORM SHAFT
8	2			THRUST COLLARS BOSTON 5C-18
9	2			3/16 DIA X 7/16 OD X 1/4" WIDE
10	7			WORM WHEEL BRONZE 48 PITCH 1.042 PD
11	2	A	96606	BOSTON G-1021
12	2	A	96607	SOCKET HD SCREW 10-32 X 3/4
13	4			HOUSING WORM GEAR
14	8			COVER GEAR HOUSING
15	12			10-32 X 1 1/4 LG. SOCKET HD CAP SCREW
16	4			#10" FLAT WASHER
17	4			1/4" RUBBER GROMMET
18	4			10-32 HEXAGON NUT
19	1	A	96608	1/2-13 X 1" HEXAGON BOLT
20	1	B	96614	1/2" LOCK WASHER
21	2			MOTOR BRACKET
22	2	A	96609	PRESSURE ROLLER HOUSING
23	2			3/16 X 1.00" DOWEL
24	2	A	96610	DRAW BOLT
25	2			SPRING COMPRESSION CLOSED 1/2" ID X 1"
26	2			FREE LENGTH .03" DIA WIRE
27	8			PRESSURE SET NUT
28	4			1/4-20 HEXAGON NUT
29	4			FLANGED BUSHING 1/2" ID X 5/8" OD X 3/4"
30	4	A	96605-2	LONG FB810-6 BOSTON
31	1	A	96611	SCREWS PAN HEAD 6-32 X 1"
32	2	A	96612	HEXAGON NUTS 6-32
33	4			#6 LOCK WASHER
34	2			3/16 DIA MAIN SHAFT
35	2			GUSSET
36	8	A	96613	GUIDE PLATES
37	6	A	96615	6-32 X 1/2 PAN HD SCREWS
38	1	B	96616	WORM DRIVE SINGLE THD HLSH
39	1	A	96617	48 PITCH BOSTON
40				3/64" X 1/4" ROLL PIN
				ROLLER END CAP
				GUIDE PINS
				SEED GUIDE BAR
				SEED CLAMP
				90° CTR SINK 2-56 X 3/16 LG SCREW

CA31266 (2 OF 2)

Figure A-3. Pull Mechanism - Ribbon Puller (Sheet 2 of 2)